FURTHER DEVELOPMENT AND TESTS OF A COLLAPSIBLE, ELASTO-PLASTIC DEFORMATION MODEL

by

Lydik S. Jacobsen[1], Alan W. Trorey[2], and Harry A. Williams[3]

Navy Contract N6eri-154, Task Order 1
(NR-064-033)

Structural Dynamics

Technical Report No. 18
August 1953.

Vibration Research Laboratory
School of Engineering
Stanford University
Stanford, California

---

1. Professor of Mechanical Engineering
2. Graduate Student in Electrical Engineering
3. Professor of Civil Engineering

ABSTRACT

This report covers the work of making the four story model, described in T. R. #17, more reliable and applicable for the experimental solution of problems involving the effects of transient disturbances on simplified structures up to their points of collapse.

Considerable difficulty was experienced in the behavior of the "plastic" elements of the model, the friction brakes. A slow, but nevertheless unacceptable time change was discovered and finally overcome. A pronounced increase in brake force or equivalent plastic resistance was found to develop as a result of the dynamic distortions. Thus if the semi-static brake force at the yield point is F_y pounds, the average dynamic brake force during yielding, F_y', follows the empirical relation:

$$F_y' = F_y(1 + 0.0015\ V_a^2)$$

in which V_a is the average distortional velocity of the story in inches per second. A simple way of controlling the magnitude of the dynamic brake force unfortunately has not been devised. Nevertheless it is believed that the indigenous behavior of the friction brakes is not much out of line with that of actual frame structures. For instance, if the average distortional velocity of the model is 10 inches per second, its dynamic, plastic resistance will be 15 per cent higher than its semi-static, plastic resistance. Since for convenient scale values a model velocity of 10 inches per second may be made to correspond to velocities of 50 to 250 inches per second in a prototype, it is conceivable that the compromises necessary in specific instances may not be too unrealistic.

Some difficulty was found in the frictional characteristics of the model and its pneumatic loaders. The inherent friction in the present design is rather high and mainly of the Coulomb type; it may be reduced to about one half of its present value by a more refined construction.

An adaptation of the present model to simulate the behavior of a building with girders of a given flexibility is possible. This aspect has been discussed in Appendix I.

The numerous tests of the model behavior covered by this report relate to fictitious, but possible prototypes. In all cases the simulation of a blast wave enveloping the model is subject to inaccuracies, not only in the shape of the pressure wave at a point, but also in assumptions about the effective areas involved. For the sake of showing trends, the propagational velocity of the prototype blast wave has been slowed down to 300 feet per second.

Four models, a one story, a two, a three, and a four story, have been tested for three mass conditions, light, medium, and heavy, and for three elastic limit strength combinations, defined by 8, 7, 6, 5 pounds, 8, 6.5, 5, 3.5 pounds, and 8, 6, 4, 2 pounds in the first, second, third and fourth stories of the model, respectively.

It is believed that our knowledge of the model's characteristics and behavior is now sufficiently precise to enable us to tackle specific or general problems with a reasonable degree of confidence in the results.

CONTENTS

INTRODUCTION

Our Technical Report No. 17, titled "Development of a 'Deformation Model' of a Building for the Study of Blast Effects" describes the design and testing of a one story pilot model; it also shows photographs of a newly constructed four story model with nine pneumatic loaders. At the time of issuing T. R. No. 17 it was believed that the four story model was ready to be adapted to specific structures for experimental studies of their blast resisting properties, but early experiments with the model last summer showed clearly that a number of improvements in its mechanical construction were desirable if the quantitative aspect of the tests had to be reliable.

This report describes the difficulties encountered and the measures taken to remedy them or to avoid them. It does not give a chronological space consuming account of our work even in cases where the time element would have been of importance in understanding why certain remedies were not tried first.

DESCRIPTION OF A FURTHER DEVELOPMENT OF THE FOUR STORY MODEL AND THE PNEUMATIC LOADERS

Frame

Referring to Figure 5 of T. R. #17, or to Figure 1 of this report, it is seen that the model frame consists of 4 units bolted together in stack formation. Each unit consists of 4 elements of Duralumin channels connected by four quarter inch steel pins accurately fitted into drilled and reamed holes. The horizontal channels are nominally 3 inches by 20 inches and weigh 2.55 pounds each; they constitute the primary mass elements of the model. The vertical channels are nominally 2 1/4 inches by 10 inches and weigh 0.47 pounds each; they may be thought of as representing the column and wall mass of a building, and they provide a means of collapsing the unit since a pin clearance of about 2/1000 of an inch enables the four elements to rotate with ease.

Restorative Elements

Collapse of an element is resisted by two spring systems, a primary or an "elastic stage" system k_e attached to the mid-points of the vertical channels and to a friction brake in which slippage can take place when the primary spring force reaches an adjustable, definite value. The secondary or "plastic" spring system k_p comes into action only when the friction brake slips; it furnishes a small positive slope to the plastic stage force function.

The actual resistance-force versus displacement function is the intrinsic restoration function minus the instability function due to the action of vertical loads on the model. Thus, if the model's height is h and its inclination with the vertical is θ, a vertical load V will produce a horizontal disturbing force of magnitude V sin θ cos θ, or approximately $V\frac{x}{h}$; consequently a negative slope of V/h defines the instability function for small values of the model's inclination, and we have $k_o - V/h$ for the actual slope of the "elastic stage", while the actual, initial slope for the "plastic stage" is $k_p - V/h$. It is thus seen that if $V = k_p h$, zero slope or constant restoring force of magnitude $(k_o - V/h)\Delta_y$ will occur at the beginning of the plastic stage. In this expression Δ_y signifies the maximum elastic distortion possible just before yielding begins.

It is, therefore, clear that not only the vertical gravity force V acting on the model, but also other types of vertical forces, as for instance a roof load, P_5, will affect the actual resistance force versus displacement curve so that in general static instability will come about when:

$$k_o\Delta_y + k_p(x - \Delta_y) = V \sin\theta \cos\theta \approx V\frac{x}{h}\left(1 - \frac{x^2}{2h^2}\right) \approx V\frac{x}{h}$$

Figures 2 to 6 show the actual restoring force-displacement relationships of the model.

Springs

Coiled primary springs of rigidity k_o have been used successfully when a relatively low stiffness is wanted, but a leaf type of primary spring, made from flat spring steel, was found more suitable than a coiled spring when relatively high stiffness is demanded. Such a spring, 5/8" wide, 3 3/8" long and 0.05" thick (See Figure 7a) has been found very suitable since its stiffness can be easily varied by adjusting the end screws to give the required moment arms. A characteristic small non-linearity in the initially flat leaf spring can be reduced to negligible proportions by having an initial curvature in the leaf spring as shown in Figure 7b. Moreover, the leaf spring offers the opportunity of being provided with SR-4 strain gauges. This is of inestimable value when a study is made of the dynamic force exerted by the friction brake itself.

The secondary or plastic stage springs are of the coiled type. Their rigidity k_p is relatively low.

Friction Brakes

The function of the friction brake is to slip when the primary spring force reaches a definite value, moreover it is desirable that the slippage force should remain sensibly constant while slipping takes place. A great deal of developmental experimentation has been done on the brake. This took place before the pilot model was made, while the pilot model was undergoing tests, reported in T. R. #17, and during the last year after the four story model had been built.

There is no doubt that a Coulomb type of friction as used in the brake is very sensitive to the condition of the slipping surfaces, and that the time-honored distinction between a static and a dynamic coefficient of friction is a reality. Our problem has been to produce a pair of slippage surfaces on which the difference between the static and the dynamic coefficients of friction is a minimum, and on which the coefficients do not vary appreciably from week to week or even from month to month.

Brake Materials Used

Eighteen combinations of the following seven brake materials have been tested: Steel, Cast Iron, Brass, Aluminum, Bakelite, Bakelite on a Linen Base, and Masonite. The combinations, Brass-Steel and Brass-Masonite gave the best results. Accordingly the four story model's four brakes were originally made of a rotating brass element and a stationary one of steel.

During our extensive testing last winter, involving the Brass-Steel brakes, it was found that over a period of weeks a steady drift toward lower values of dynamic brake resistance took place, so that, even if the brakes had been statically calibrated before each test, the permanent sets obtained differed greatly in tests made days and weeks apart, indicating that time changes in the dynamic behavior were taking place.

Permanent Sets are Sensitive to Brake Performance

It is of importance to realize that in a multi-story model,

exposed to a given transient loading, the "plastic" strength distribution, story by story, is of great consequence in determining the plastic configuration of the model for large permanent sets. This is especially true for the lower stories in which the gravity load due to the upper stories often is responsible for a negative slope of the plastic-resistance versus deflection curve. Since near-collapse is usually localized in one story, its plastic strength becomes to a large degree the determining factor for permanent sets. Nevertheless, the distortions of all stories will enter into the picture since their individual motions affect the effective forces.

The Brass-Steel Brakes

In our four story model with Brass-Steel Brakes three "identical" tests, made one and two weeks apart, gave the following average permanent displacements:

	1st	2nd	3rd Test.
First story	1.05"	1.50"	1.60"
Second story	.9	1.3	2.30
Third story	.95	1.45	2.35
Fourth story	.9	1.55	2.30

Since from the point of view of a static setting of the friction brakes the model was in the identical condition for the three tests, the differences in its behavior had to be ascribed to dynamic changes taking place in the brakes over a considerable time. Thus, when four tests were carried out

on the same day the following permanent displacements were:

	1st	2nd	3rd	4th Test.
First story	1.55"	1.65"	1.35"	1.58"
Second story	2.35	2.52	2.25	2.33
Third story	2.36	2.52	2.27	2.32
Fourth story	2.36	2.55	2.23	2.32

This shows that within the accuracy of observation no permanent sets occurred in the third and fourth stories, and that a time change for one day was not clearly discernible. The maximum spread of the first story set was 0.30 inches while the maximum spread of the second story set was 0.15 inches. In view of the relatively large distortions involved the above data was consistent enough, but the long time effect remained.

Another difficulty with Brass-Steel brakes occurred when their semi-static calibrations were made. The force versus displacement records showed a saw tooth shape for distortions above the elastic limit. Various lapping techniques were tried, but none was found that would prevent the chatter. Application of "Molycote Z" graphite seemed to be effective against chatter for a short time, but the drift of the brakes toward lower resistances remained a serious defect.

Brass-Masonite Brakes

It was then decided to return to the Brass-Masonite combination, retaining the rotating brass elements and "lining" the steel elements with 5/32 inch thick Masonite plate of the hard

pressed type. A technique was finally developed for lapping the Brass-Masonite surfaces in place by using a relatively coarse valve grinding compound, "Cloverleaf", Grade C, thereby producing visible, concentric, circular markings. The lapping compound was then cleaned off with CCl_4. After the lapping and cleaning off process had been repeated two or three times with a fine lapping compound, U. S. Products Co., grade $302\frac{1}{2}$, a further lapping without any compound followed for several minutes. Before testing was begun a final "lapping" with graphite powder was done. The excess graphite surrounding the friction surfaces was then blown off and a careful cleaning with CCl_4 left the thin graphite film on the friction surfaces undisturbed.

Extensive testing of the Brass-Masonite brakes showed that they are dynamically stable for an indefinite length of time and that practically no chattering takes place. So many tests were made, (138), that the concept of a standard deviation begins to take on a meaning. For large permanent sets of 1.5 inches and above, as are likely to occur in the lower two stories, the standard deviation is 0.17 inches, while for permanent sets in the upper two stories the standard deviation is only 0.04 inches.

The dimensions of the four flat friction surfaces in a brake are 2 inches in outer diameter and $1\frac{9}{16}$ inches in inner diameter, giving a total contact area of about 2 x 1.2 square inches. The coefficient of friction is in the order of 0.40 when the surfaces are pressed together with a force of 90 pounds; the force resulting

from compressing a 75 pounds per inch coiled spring by a nut making about 22 turns. Therefore, each turn of the nut produces a friction force of about 90/22 x 0.4 or 1.6 pounds. Since the brake elevation and primary spring connections are located at one half of the story height, the slippage force at the story height is about 0.8 pounds per turn of the compression nut. It should be stated here that the coefficient of friction is definitely a function of the pressure on the surfaces and that the brakes cannot be set to a sufficient degree of precision by making use of the linear relation between pressure and number of turns of the pressure nut. Dead-weight calibration or a semi-static, steady pull through a dynamometer were the original methods used for setting the brakes. By reasonable care it is possible to set the brakes to an accuracy of $\pm$ 0.02 pounds.

Dynamic Constancy of Brakes

The question of the constancy of the Brass-Masonite friction brakes under dynamic loadings was not answered until recently, June 1953, when the leaf type of primary spring had been developed and SR-4 strain gauges could be attached directly to the springs. Semi-static as well as dynamic experimentation has now shown that the initial slippage force - the "elastic limit" force - together with the continued slippage force - the "plastic" force - are increased somewhat by having dynamic distortions instead of semi-static ones. When an initial slip begins, the slipping velocity of the brass element will be proportional to the distortional

velocity of the story if the inertia effect of the brass element is vanishingly small. Since this is the case for the dimensions of the brake used, we can plot the average dynamic brake force F_y' against the average slipping velocity V_a. The following empirical relation has been found:

$$F_y' = F_y(1 + 0.0015\ V_a^2)$$

in which F_y is the semi-static "yield" or "elastic limit" brake force, and V_a is in inches per second, see Figure 36. Thus, for a distortional or slipping average velocity of 10 inches per second a 15 percent increase in brake dynamic force will result. This situation is acceptable since it is in qualitative harmony with the experimental fact that most materials show increases in strength for rapid loadings. The empirical relation is satisfactory up to about 25 inches per second distortional velocity of a model story. It is, of course, regrettable that a quantitative control of the brake dynamic forces cannot be exercised.

For purposes of estimating the dynamic brake force F_y' from the final distortions Δ, the empirical formula

$$F_y' = F_y(1 + 0.04\ F_y\ \Delta),$$

in which Δ is in inches and F_y is in pounds, may be used with reasonable accuracy up to $\Delta = 2.5$ inches (See Figure 35).

The whole problem of correlating dynamic increases in brake forces of the model with dynamic increases in the resistance of building materials has not yet been answered; all that can be said at the present is that the Brass-Masonite combination offers

this possibility since its dynamic coefficient of friction is larger than its static.

THE DYNAMIC LOADERS

Cylinders

The original loaders described in T. R. #17 have worked reasonably well. Carefully turned Magnesium pistons of 1.125 inch diameter and 1.25-inch length slide in cylinders of 1.127 inch diameter, and 9.15 inches long, making the cylinder volumes vary between a maximum of about 8 cubic inches and a minimum of 1.8 cubic inches. The pistons, weighing 0.02 pounds, are connected by hollow Duralumin rods, weighing between 0.005 and 0.015 pounds, to ring-dynamometers carrying four strain gauges. All connections are by home-made ball and socket joints. The weight of the ring-dynamometer is close to 0.13 pounds, and its rigidity is in the order of 600 pounds per inch. Consequently, the natural frequency of the dynamometer, connecting-rod, piston system is in the order of 250 cycles per second.

Storage Cylinders

Adjustable air storage flasks or cylinders, 2 $\frac{3}{8}$ inches in diameter by 9 $\frac{1}{4}$ inches long, can have their volumes varied from approximately zero to 36 cubic inches by adjustably located pistons. For ordinary operation about 8 cubic inches of storage volume is used. The storage cylinders as well as the loader cylinders were obtained from surplus hydraulic gear used on obsolete aircraft.

The method of operating the dynamic or pneumatic loader is to charge its corresponding storage cylinder with air at a given pressure, then to discharge it suddenly into the loading cylinder. The suddenness of opening a ball-valve, the dimensions of the ball-valve and connecting conduit, and the initial volumes and pressures of the storage and loader cylinders are the principal factors influencing the early history of the transient loading phenomenon. Its later history depends also on the rate of bleeding and on the motion of the loader piston. Further control is obtained by having a throttle-valve in the connecting conduit and a pop-off valve with adjustable mass weights communicating with the loader cylinder.

Piping

The rapidity of pressure rise in the loader cylinder depends to a large extent on the size of the piping connecting the two cylinders as well as on the size and method of operating the ball-valve. The connecting piping is the ordinary 1/4 inch type, about 19 inches long with an effective volume between storage and loading cylinder of somewhat more than 1 cubic inch.

Ball-Valves

Figure 8 shows a sketch, and Figure 9 shows a scale drawing of the solenoidally operated ball-valve, originally designed by Dr. R. S. Ayre. An O ring, rubber gasket enables the $\frac{3}{8}$ inch diameter steel ball to form an excellent seal. The 5/64 inch diameter push rod, rapidly actuated by the solenoid plunger, shoves the ball

against the storage pressure thereby opening a passage for the air confined in the storage cylinder to flow through the conduit into the loader.

Throttling and Bleeding

If it is desired to throttle the flowing air so as to obtain a slower rise time in the loader, a 1/4 inch needle valve with a 5/32 inch opening is located in the conduit and can be adjusted by a screw thread of 1/20 inch pitch.

The bleeding-valve connected to the loader is also a 1/4 inch needle valve. It discharges through a pop-off valve into the open air.

The Pop-Off

The pop-off valve consists of a 1/4 inch diameter brass rod located in a 17/64 inch diameter vertical cylinder. The rod seats under the influence of gravity over a 3/16 inch hole located directly above the throttle valve. As the air pressure builds up below the rod, it starts to lift it off the seat, blowing air through the 1/64 inch diametral clearance space of rod and cylinder. As the rod rises it suddenly uncovers two 3/16 inch horizontal vent holes located 7/16 inch above the rod's seat. The inertia of the rod carries it somewhat past the vent hole position where it is arrested and held by a clip spring. By using rods of different lengths the initial lifting pressure and the vent uncovering time element can be changed. The weight of the smallest rod was 0.014

pounds, the largest 0.17 pounds. If no pop-off is desired the rod is removed or simply left in its upper spring held position.

Gages

Inexpensive Bourdon gages, U.S.G. 10946-1, with 1.7 inch hands divided the pressure range 0-100 psig. into an arc of approximately 300 degrees. Better gauges are recommended.

Thermal time effects are especially noticeable in the storage cylinders. Thus when they are charged up to 50 psig. fairly rapidly and then closed off, the pressure falls as much as 15 psig. during an interval of 20 seconds. Conversely, when they are discharged rapidly from 50 psig. and the solenoidally operated ball-valve closes them off again within one third of a second, the pressure in a "discharged" storage cylinder may rise as high as 15 psig.

FRICTION IN THE MODEL

Original Friction Values

When the nine loaders are disconnected from the four story model nearly all the friction during an elastic vibration of the system is due to the 16 pin joints used for assembling the frame and the 8 pin joints used for fastening the primary springs to the frame. The friction is therefore predominantly of the Coulomb type, and the slope of the almost straight line envelope of the displacement versus time curve at the "cease motion point" gives a fair measure of the friction forces involved. For a definite speed of the recording paper it was found that the envelope's slope was - 0.42 when no loaders were attached, while it was - 1.09, and still a reasonably straight line, when all nine loaders participated in the motions at their respective locations on the model. Consequently, the nine loaders produced a negative slope of the envelope equal to 0.67, or they accounted for about 60 percent of the total friction of the system.

For purposes of comparison, a four story model, vibrating in its fundamental mode, may be thought of as being equivalent to a single mass oscillator. The frictional work done at the pin joints of the model's frame may then be assumed to be proportional to the distortional displacements of each story as well as to the loads on the joints. On the pin joints of the primary springs only horizontal forces of about 40 lbs. are acting due to the initial spring tensions; on the frame pins horizontal forces of about 20 lbs.

due to spring tensions as well as vertical forces due to the model's weight become effective. Considering that the story distortions (beginning at the top and progressing toward the ground) are relatively: 10, 18, 30, and 42 percent of the top story's displacement, when the model vibrates in its fundamental mode, we find that the frictional work done at the six joints of each story will be 8, 16, 30, and 46 percent of the total frictional work respectively.

Magnitude of Frictional Forces in Frame

The free vibration records of the four story model without pneumatic loaders attached show that for an initial 4th story amplitude of 0.65 inches, the model comes to rest in 3.2 complete cycles. This means that the original frictional forces per story are: 0.11, 0.20, 0.37, and 0.53 pounds respectively.

Careful cleaning, oiling and alignment of the 24 pin joints reduced the displacement envelope slope of the model without loaders to the value - 0.39, a rather small change of 7 percent.

The only promising way of decreasing the pin friction is to use high grade ball bearings, necessitating two for each pin, or 48 in all. This change can be effected if desired, but it makes the model considerably more involved and therefore has not been tried so far.

Magnitude of Frictional Forces due to Loaders

Unlike the pin joints, where the frictional work is due to

distortion, the loaders, being attached to a story and having their cylinders fixed to the ground, introduce frictional work due to the absolute displacement of each story. Consequently the fundamental mode vibration of the four story model with absolute displacements proportional to 1.00, 0.90, 0.72, and 0.42, will dissipate for equal loader resistance per story 33, 29, 24, and 14 percent of its frictional work at the four different stories.

The free vibration records for the four story model with 9 loaders attached, with 7, 5, 3 loaders, and finally with the roof loader only, bear out the reasoning that the frictional work is proportional to the absolute displacements of each loader. This gives an original frictional force of 0.88 pounds for the three top story loaders, a force of 0.50 pounds for the two third story loaders, 0.41 pounds for the two second story loaders, and 0.22 pounds for the two first story loaders. Seemingly the frictional effect of the roof loader is about equal to the effect of one of the horizontal loaders at the 4th story.

Very careful cleaning and polishing of pistons and cylinders with crocus cloth, followed by cleaning with carbon-tetrachloride, reduced the friction due to the nine loaders so as to give a free vibration envelope slope of - 0.90. This means that the slope - 0.90 - (- .39) = - 0.51 is due to the loaders, and the corresponding friction force per loader is reduced to 0.22 pounds at the top story, 0.19 pounds at the third, 0.16 pounds

at the second, and 0.08 pounds at the first story. A reduction in friction of 24 percent due to cleaning and polishing alone.

It is seen that the total friction force per story due to lubricated pin joints and to clean loaders adds up to approximately the same value, namely: 0.75, 0.57, 0.66, and 0.66 pounds per story respectively.

Study of Piston Friction

The tests have shown that even in the clean condition the loaders are responsible for more friction in the four story model than are the pin joints. A study of the piston friction therefore has been undertaken.

The presence of the ring dynamometer with its strain gauges in the loader system greatly facilitated observation of frictional forces acting on the piston since the electrical signal from the dynamometer could be recorded along with a forced or a free vibration displacement of the model. In order to simplify the study the three lower stories were clamped, and the top story, without any loader attached, was used as the basic comparison for tests with a single loader. The dynamometer record therefore includes: the inertia forces due to the motion of the piston, connecting rod, and part of the dynamometer, the cylinder air force due to the motion of the piston, and the piston friction force. A small amount of "hash" is due to the unavoidable clearances in the two ball and socket joints, one of which connects the piston to the rod, while the other connects the dynamometer to the frame of the model.

A free vibration of the top story without loaders attached makes 14 complete cycles before coming to rest if the initial amplitude is 0.25 inches. This gives a constant friction force of 0.12 pounds for the one story model, a value in fair agreement with the force of 0.11 pounds obtained originally for the first story of the four story model.

Oiling of Pistons

When "3 in 1" lubricating oil was used on the loader pistons a very great increase in damping occurred, approximately cutting in half the number of swings leading to a "cease motion". In view of the relatively small radial clearances of the pistons, 1/1000 of an inch, this behavior was to be expected.

Graphite on Pistons

Application of "Molycote, Z" powdered graphite to the cleaned pistons and cylinders of the loaders reduced the negative slope of the displacement versus time record from 0.90 to 0.85. Consequently the inherent friction in the oiled pin joints of the model causes a slope of - 0.39 and the nine clean and graphite lubricated loaders are responsible for the additional slope of - 0.46. The graphite also acts as a protection against oxidation.

Air Pumping Effect

The friction effect due to the air "pumping" of the loader piston in the cylinder with full bleeding was found to be negligible. This has been determined by removing the cylinder head. In

fact, with the bleeding cut off so as to make the cylinder into an air spring, the frequency of the model was slightly increased, but the friction was not changed enough to be observed.

Counterweighting of Pistons

A long, vertical string was attached to the connecting rod as near to the piston end as the cylinder allowed. The vertical pull in the string was then varied in small steps by extending a soft spring in series with the string so as to lift the weight of the piston. Free vibration friction records taken for string pulls, varying between zero and a value large enough to reverse the gravity pull on the piston, showed a minimum value of friction for a given pull. This minimum friction force amounted to approximately one half the value of the loader system without a counterweighted piston, indicating that a counterweighting scheme of the eight horizontal loader pistons might reduce the Coulomb type of friction produced by the nine loaders to give a displacement record slope of approximately -0.30, equivalent to a total loader force of about 0.90 pounds.

Since the counter weighting is quite sensitive to the string pull, and since the eight long strings would be in the way during experimentation, it was decided to leave the loaders without counterweights for the present.

Possible Reduction of Friction

If it should be found desirable in the future to reduce the

friction in the loaders, the counterweighting method offers an opportunity of obtaining approximately four cycles of free vibration following an initial displacement of one inch at the 4th story. A rebuilding of the model's frame, using high grade ball bearings on all pin joints, might then be expected to reduce the pin friction to about one fourth of its present value. In that case the four story model would probably execute slightly more than five cycles of free vibration following an initial displacement of one inch at the 4th story, a performance that may be compared with the present one of slightly more than two and one half cycles.

In most of the tests carried out on the model and described in this report, plastic deformations were so large that the presence of pin joint and pneumatic loader friction was not strongly objectionable. This, however, will not be the case if tests involving relatively small permanent sets are to be contemplated.

CONSTANTS OF THE FOUR STORY MODEL

Weight of mass per story		9 lbs	12 lbs	15 lbs
Primary spring stiffness per story, k_o		27 lbs/in	27 lbs/in	27 lbs/in
Primary stiffness per story considering gravity effect	Fourth	26.1	25.8	25.5
	Third	25.2	24.6	24.0
	Second	24.3	23.4	22.5
	First	23.4	22.2	21.0
Secondary spring stiffness per story, k_p		1.7	1.7	1.7
Initial, secondary stiffness per story considering gravity effect.	Fourth	0.8	0.5	0.2
	Third	-0.1	-0.7	-1.3
	Second	-1.0	-1.9	-2.8
	First	-1.9	-3.1	-4.3

The single story model is obtained by clamping the first, second, and third stories, the two story by clamping the first and second stories, etc.

Natural Frequencies of One to Four Story Models

Single Story		5.33	4.59	4.08
Two Stories	Fundamental	3.25	2.79	2.46
	Second mode	8.58	7.37	6.54

Three Stories	Fundamental	2.31	1.98	1.75
	Second mode	6.56	5.62	4.79
	Third mode	9.51	8.14	7.19
Four Stories	Fundamental	1.79	1.53	1.33
	Second mode	5.21	4.55	3.96
	Third mode	8.19	7.16	6.23
	Fourth mode	9.81	8.57	7.45

MODEL - PROTOTYPE RELATIONSHIPS

Single Story Model

Let the height of the story be $h = 10$ inches

the primitive, primary elastic stiffness, $k_o = 27$ lbs/inch

the primitive, secondary plastic stiffness, $k_p = 1.7$ lbs/inch

the equivalent weight of the story's mass $w = 9$ pounds

The natural period of the model is then

$$T_m = 2\pi\sqrt{\frac{w/g}{k_o - w/10}} = 2\pi\sqrt{\frac{0.0233}{26.1}} = 0.1877 \text{ seconds.}$$

Dimensions and Properties of Prototype

Let the story height H be 12 feet. This means that the length scale λ is H/h or 14.4. On the basis of equal angular deformations in model and prototype (see T. R. #17) the time scale τ must be equal to the square root of the length scale.

$$\tau = \sqrt{\lambda} = 3.79$$

Similitude also requires that the natural period of the prototype must be equal to T_m multiplied by the time scale τ, or

$$T_p = \tau T_m = 0.712 \text{ seconds.}$$

Let the equivalent weight W of the prototype be 18,000 pounds. This means the weight, mass, and force scale μ is W/w or 2000. Consequently the primitive elastic stiffness K_o of the prototype must be

$$K_o = \frac{4\pi^2 \mu w}{T_p^2 g} + \frac{\mu w}{\lambda h} = \frac{4\pi^2 46.6}{0.712^2} + \frac{18{,}000}{144} = 3640 + 125 = 3765 \text{ lbs/inch}$$

The stiffness scale σ is therefore $K_o/k_o = 139.5$, and the primitive plastic stiffness of the prototype is $\sigma K_p = 237$ lbs per inch.

Force Actions on Model and Prototype

A static horizontal force of 3640 pounds will displace the prototype one inch, and a static force of $3640/\mu$ or 1.82 pounds will displace the model

$$\frac{1.82}{26.1} = \frac{1}{14.4} = \frac{1}{\lambda} \text{ inches}$$

A peak dynamic force of 26 pounds acting on the model will correspond to a peak dynamic force of $\mu 26 = 52$ kips acting on the prototype.

If the frontal area of the prototype is 12 feet x 20 feet, and if one half of the blast load is assumed to be carried by the frame of the prototype, the peak, blast load pressure will be 433 pounds per square foot or 3.0 pounds per square inch.

If the model's brake force F_y is arbitrarily set at the semi-static value of 5 pounds, the corresponding yield force of the prototype will be $\mu 5 = 10$ kips.

A final displacement Δ of say 1.5 inches of the model will mean a final displacement of $\lambda 1.5 = 21.6$ inches of the prototype. The corresponding permanent sets of the model and the prototype are then

$$1.5 - \frac{w}{k_o} = 1.167 \text{ inches and } 21.6 - \frac{\mu w}{\sigma k_o} = 16.82 \text{ inches}$$

respectively, the length ratio λ being preserved.

If the test record shows that the average distortional velocity V_a of the model is 14 inches per second, the corresponding average distortional velocity of the prototype will be 14 λ/τ or 14 x 3.79 = 53 inches per second.

An estimate of the dynamic brake force of the model may be made from the experimental curves, Figure 35 and Figure 36. For V_a = 14 inches per second as well as for Δ = 1.5 inches we obtain 6.5 pounds instead of the semi-static setting of 5 pounds. This corresponds to a 30 percent increase in yield strength of the prototype due to dynamic causes.

Assuming that the length of the roof of the prototype in the direction of the blast wave propagation is 24 feet, the wave front traveling at the rate of say 1200 feet per second will have moved across it in 20 milliseconds. The corresponding travel time on the model will then be $20/\tau$ = 20/3.29 = 5.38 milliseconds. It should be noted that the physical length of the model does not enter into consideration, since the "length" of the model may be defined by a time delay in the roof loader. A force pulse of 100 milliseconds duration acting on the model corresponds to a pulse of 379 milliseconds acting on the prototype.

Four Story Model

Retaining the dimensions of the single story model and stacking four such units, we note that the effective elastic stiffnesses become:

23.2, 24.3, 25.7, and 26.1 pounds per inch

while the effective plastic stiffnesses assumed the values

-1.9, -1.0, -0.1, and 0.8 pounds per inch.

The four natural periods of the model may then be calculated by standard methods. They are

0.560, 0. 192, 0.122, and 0.102 seconds.

Assuming for the prototype the same story heights and equivalent weights as used in the single story example, it is easily shown that the required natural periods of the prototype, τT_m etc., or

2.12, 0.729, 0.463, and 0.387 seconds

will be obtained if the stiffness scale Δ remains 139.5 as before and if the primitive elastic stiffness of each story is 3760 pounds per inch. The effective elastic stiffnesses of the prototype are then

3240, 3390, 3520, and 3640 pounds per inch

while the effective plastic stiffnesses become

-265, -140, -14, and 112 pounds per inch.

Timing of Loaders

The simulation of a blast wave enveloping the model by a finite number of loaders is inaccurate in several respects, mainly due to the causes:

a) Concentration of horizontal forces

b) Concentration of roof forces

c) Shape of loader forces with time

d) Timing of roof and rear wall forces

Assuming that the prototype may collapse as a whole, but that local failures do not occur, it is believed that causes a) and b) are not serious. The shapes of the force-time curves, c), are of some importance, but great accuracy in detail is probably not necessary. Cause d), the timing of the various loaders, is admittedly of importance.

The four front loaders must be timed together, but the roof and rear wall loaders present some difficulties in timing since they must simulate a traveling time-disturbance at localised stations. This means that the pressure integrated over a variable area must be concentrated, as a function of time, at a fixed location.

If the duration of the pressure pulse is relatively long in comparison with the time it takes the disturbance to envelop the structure, all the force loaders of the model may be fired simultaneously. They will then impress on the model the same force-time function as the given pressure-time function. In our experiments the pressure pulses used on the roof and back of the model endure for a minimum of 100 milliseconds while the travel time of the disturbance over the roof takes from 6 to 10 milliseconds for the model-prototype relations used in the example. Consequently the timing of the loaders should be almost simultaneous.

On the other hand, if the pressure pulse duration is very short, the roof area involved becomes a function of time, increasing to a maximum area smaller than the total area. Then the

pressure integrated over this maximum area travels over the length of the roof until it reaches the rear corner after which the area diminishes to zero. In this case a localized roof loader force should increase to a maximum, then remain constant and finally diminish to zero.

In view of the desirability of getting a clearer picture of the enveloping time effect of a pressure pulse than otherwise possible, we have exaggerated the timing delays used in the tests to correspond to a prototype of approximately four time the dimensions of the one otherwise simulated by the model. A different way of stating this situation is to say that we have assumed a disturbance propagation velocity of 300 feet per second of a wave enveloping the prototype. See Figure 18 for the loadings used in the experiments.

FIGURE 1

Showing the four story model construction simulating a four story prototype with infinitely rigid girders.

In the Appendix I, Figure 39 shows a modification of the model whereby it may be made to simulate a prototype having girders of finite rigidity.

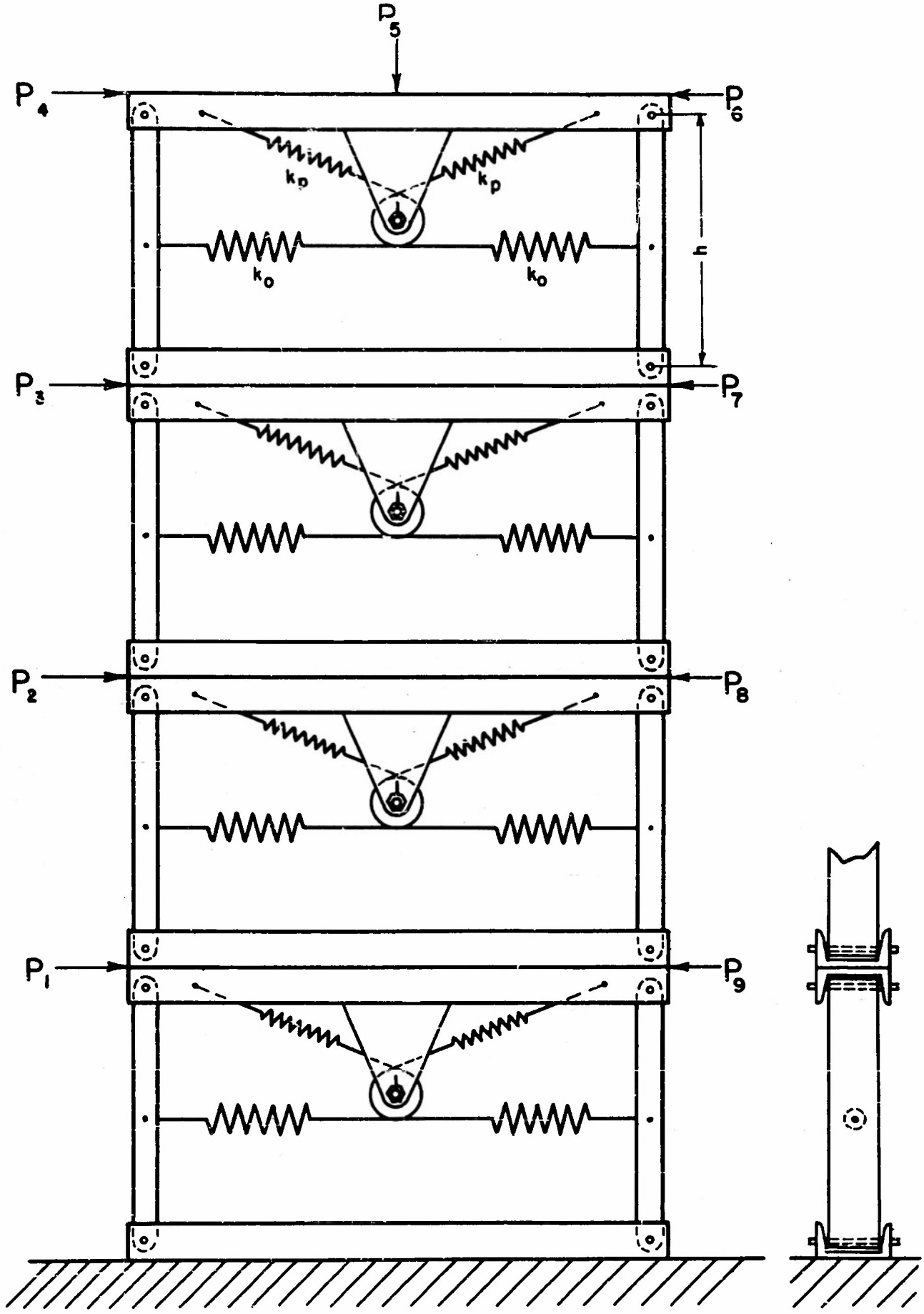

FIG. 1

FIGURE 2

Showing the intrinsic elastic - plastic restoring force

$$k_o \Delta_y + k_p (h \sin \theta - \Delta_y)$$

and the instability force due to the vertical force V

$$\frac{1}{2} V \sin 2\theta$$

The restoring force is drawn for an elastic limit deflection, $\Delta_y = 0.341$ inches, corresponding to an elastic limit force of 8 pounds for the model weighing 9 pounds per story.

The instability force is shown for the first story when the total weights are 60, 48, and 36 pounds.

The intersections indicate that static collapse occurs at $\theta = 12^\circ$ or at $\Delta = 2.07$ inches (see Fig. 6) for the 60 pound model, and at 17.5° or $\Delta = 3.45$ inches for the 48 pound model, while no collapse is possible for the 36 pound model.

FIGURE 3

Restoring force-displacement curves for the one story model with $F_y = 2$ pounds and different model weights as shown.

The 9, 12, and 15 pound curves are straight lines to a high degree of approximation.

FIGURE 4

Restoring force-displacement curves for the bottom story of the two story model with $F_y = 4$ pounds for the 36 pound model.

The non-linearity of the plastic region curves begins to be noticed. The 30-pound model will collapse at $\Delta = 3.85$ inches.

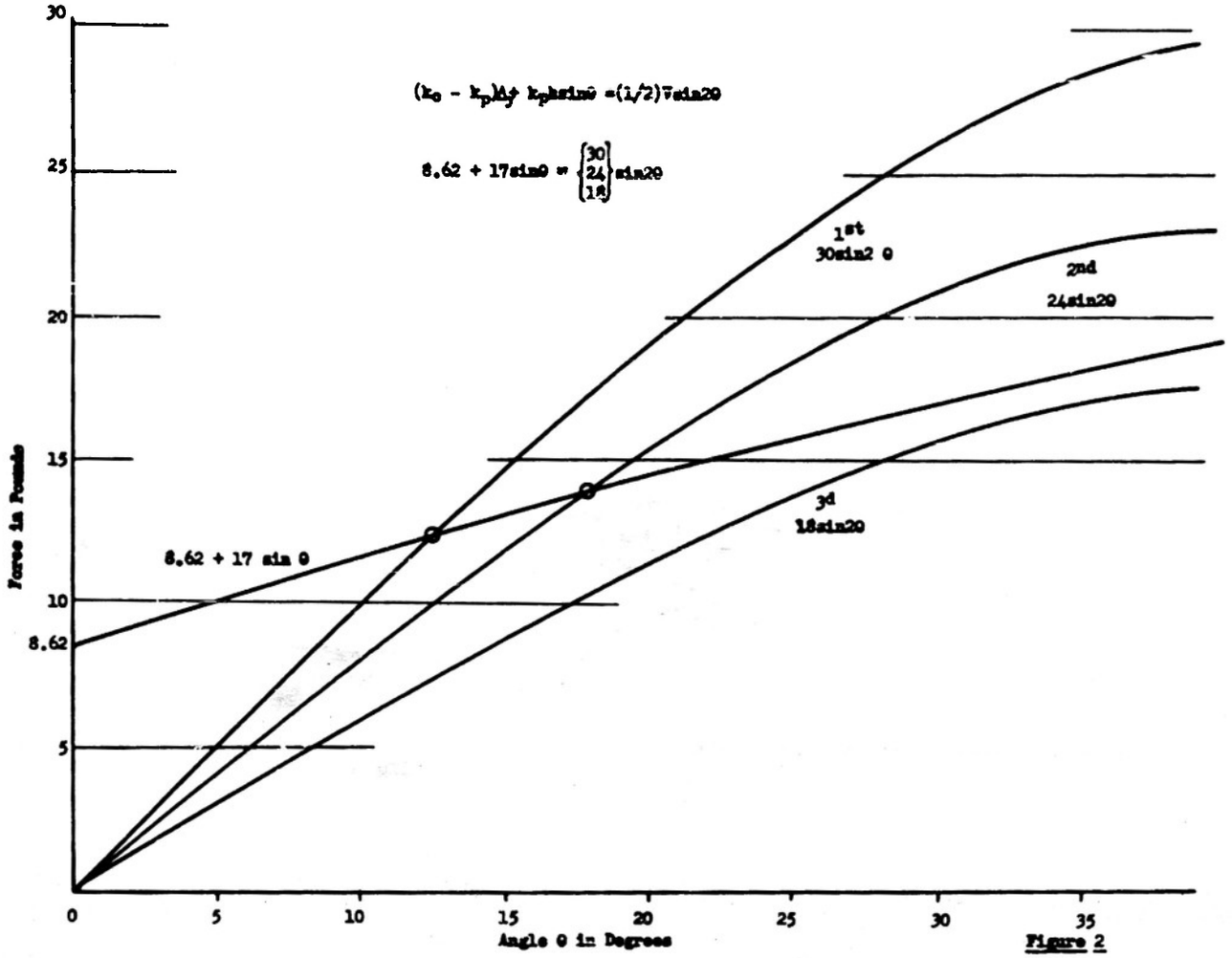

Figure 2

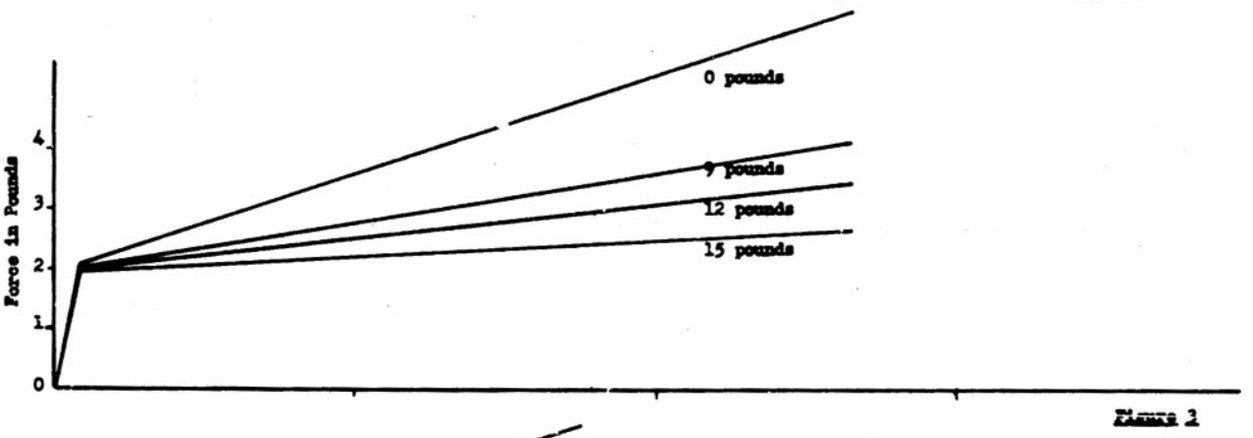

Figure 3

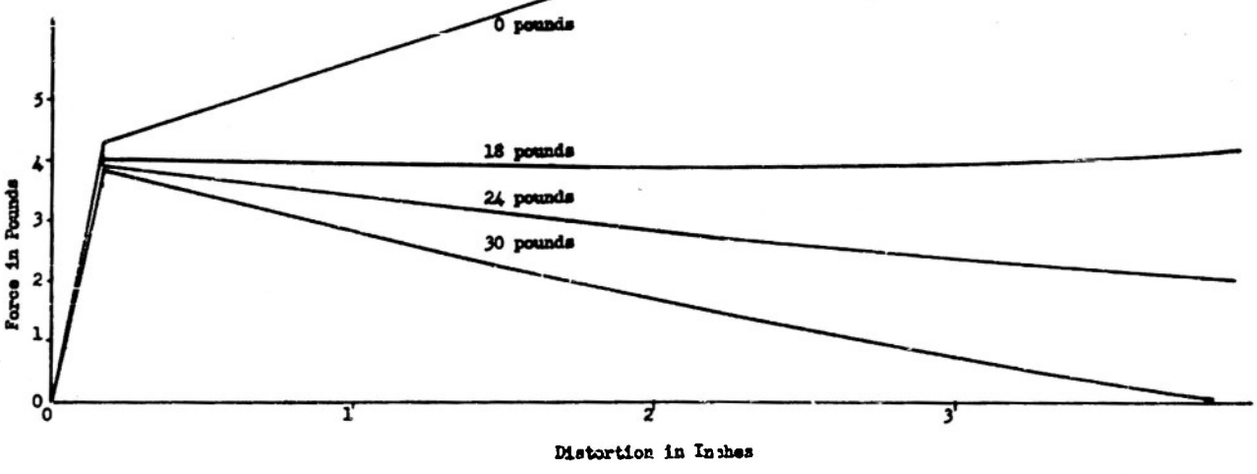

Figure 4

FIGURE 5

Restoring force-displacement curves for the bottom story of the three story model with F_y = 6 pounds for the 36 pound model.

The intrinsic elastic-plastic curves have been marked 0 pounds. Collapse of the 45 and 36 pound models will occur at Δ = 2.47 and 3.92 inches respectively, while collapse of the 27 pound model is not possible for the given value of k_p.

FIGURE 6

Restoring force-displacement curves for the bottom story of the four story model with F_y = 8 pounds for the 36 pound model.

Collapse of the 60 and 48 pound models will occur at Δ = 2.06 and 3.45 inches respectively. The 36 pound model will not collapse.

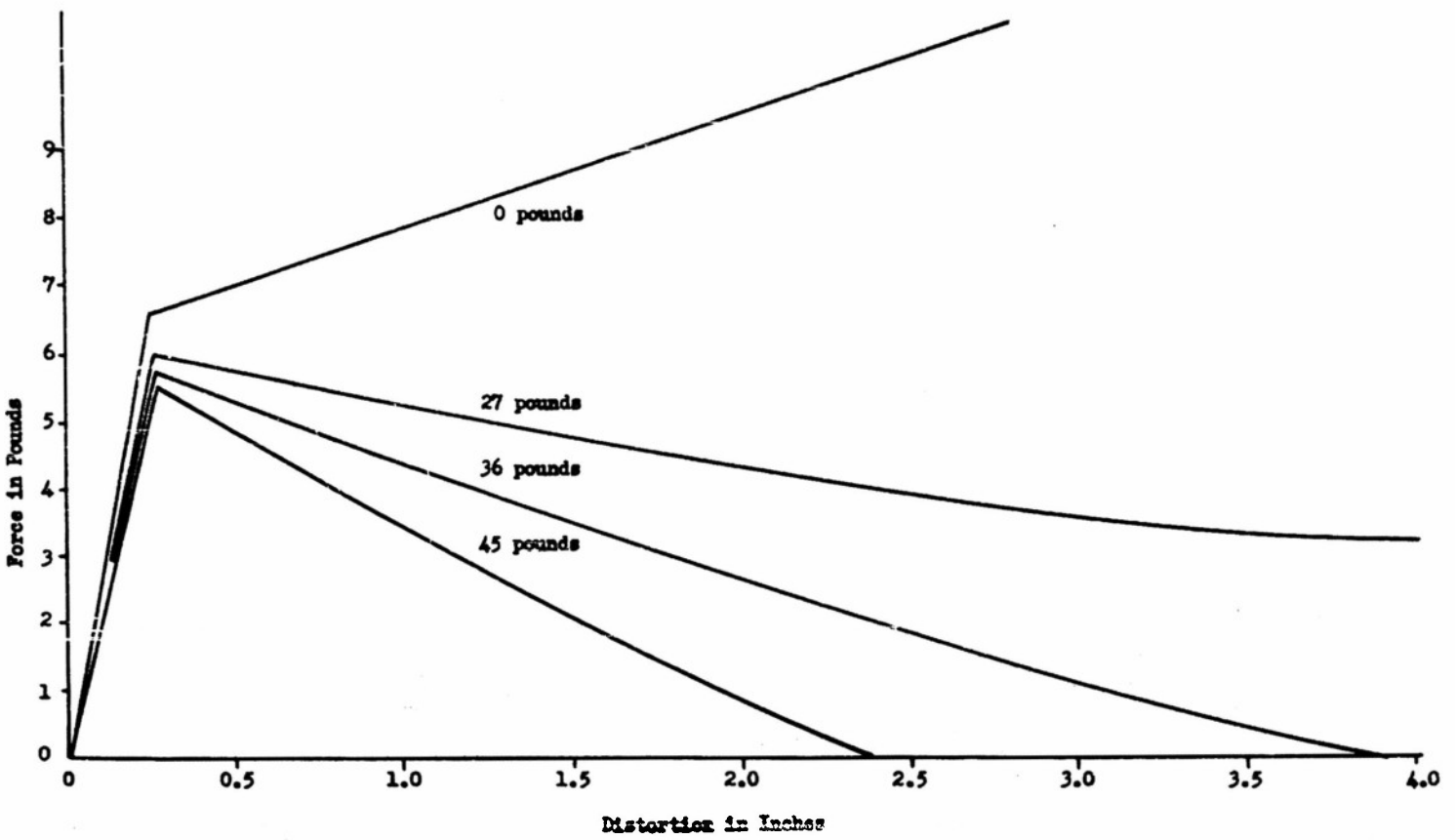

Figure 5

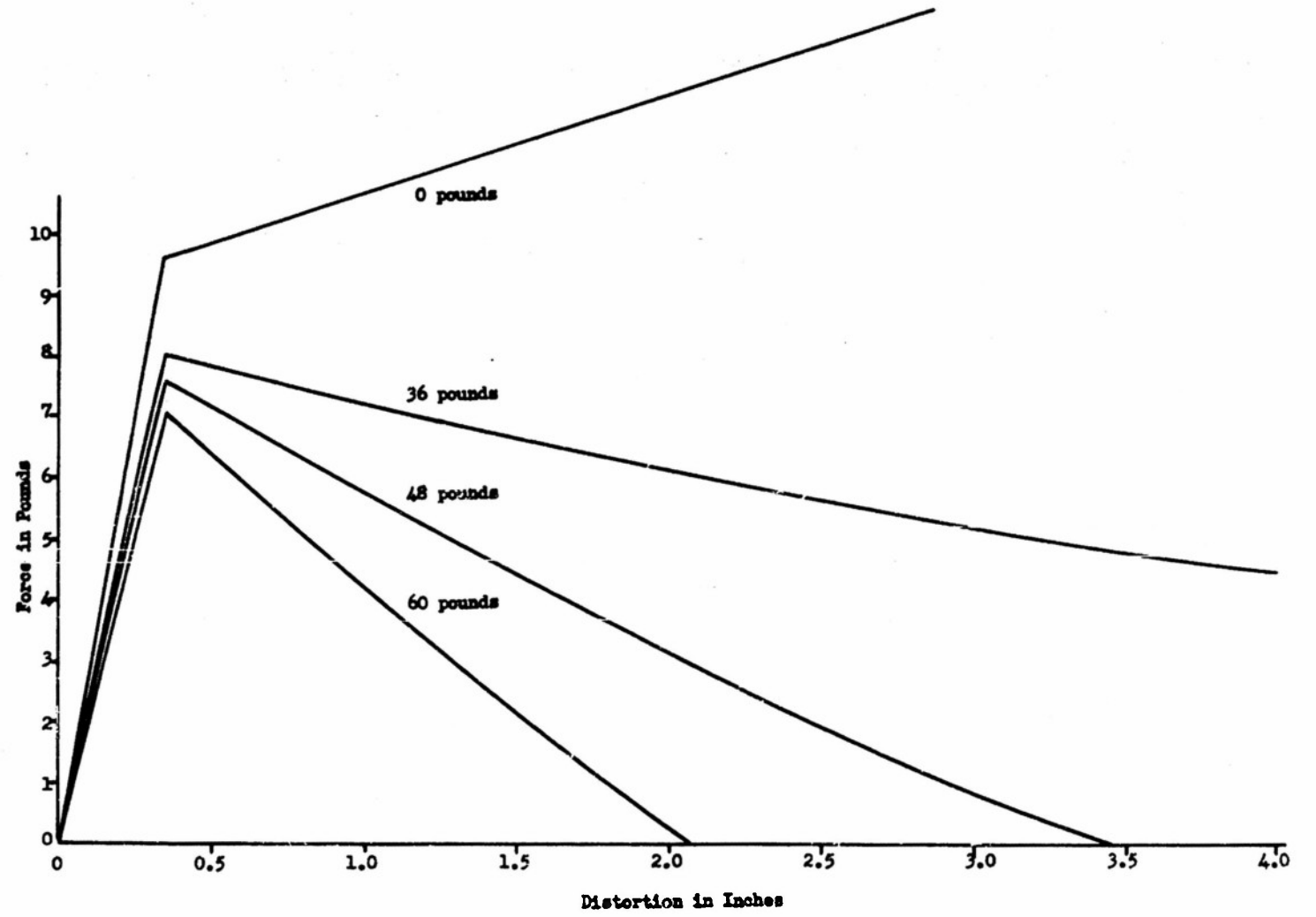

Figure 6

FIGURE 7

a) Showing the leaf spring design, under load, used for the primary spring system in the later experiments of this report.

b) Showing the unstressed shape of the leaf spring. The initial load straightens the spring and thereby improves the linearity of its stiffness characteristic at the operating loads.

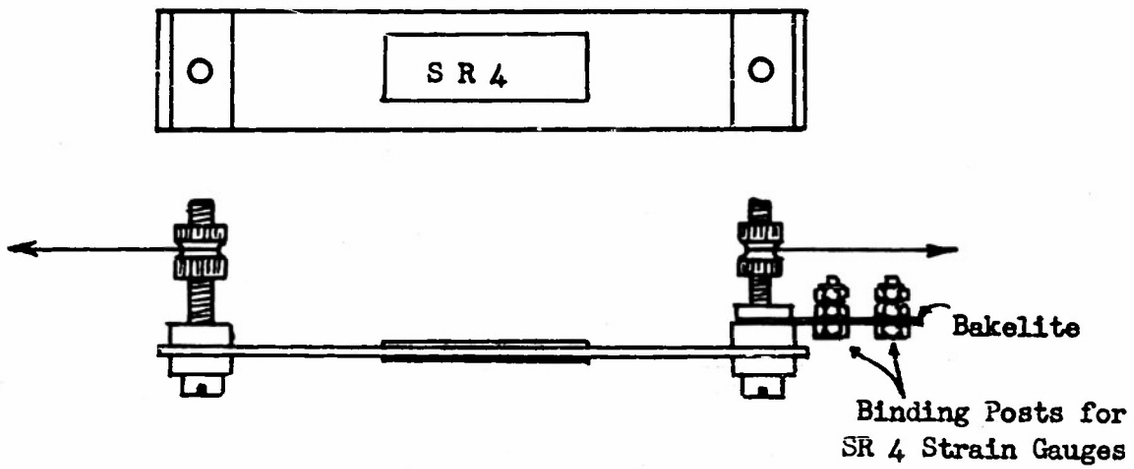

(7a)

(7b)

Figure 7

FIGURE 8

Assembly drawing of the air valve used in the pneumatic loader system.

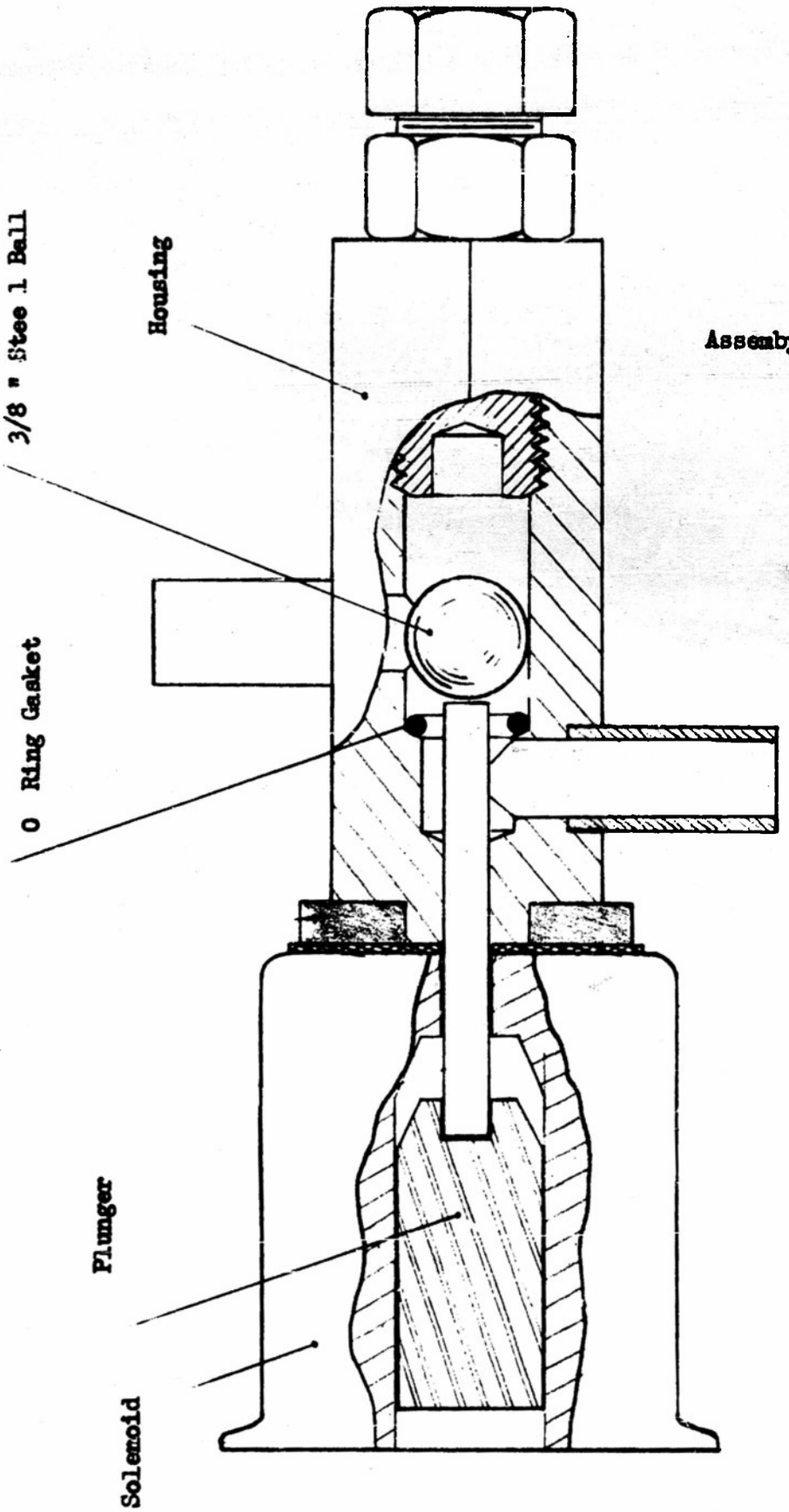

Assemby Drawing of Air Valve

Figure 8

FIGURE 9

Detail drawing of the air valve.

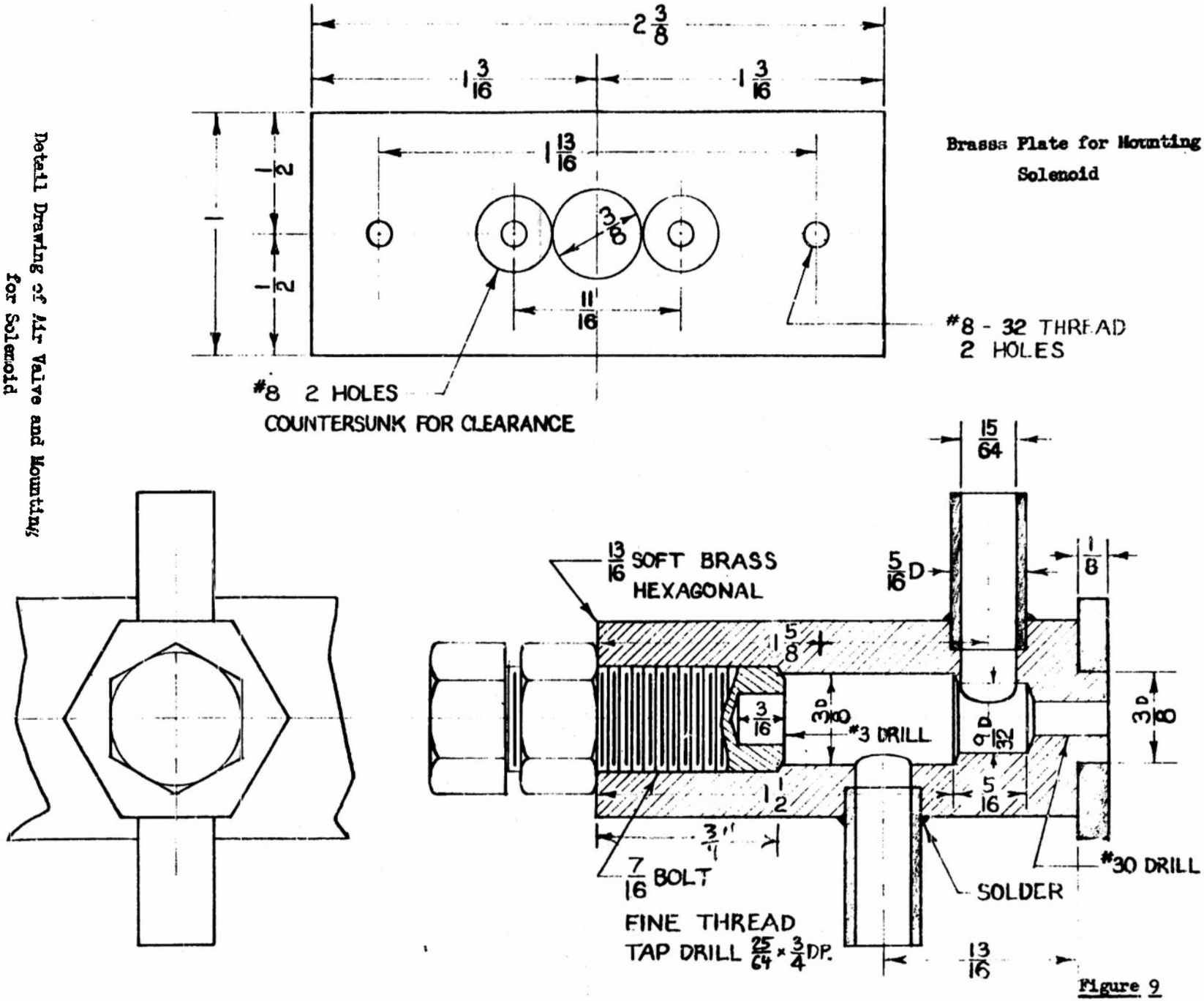

Figure 9

Detail Drawing of Air Valve and Mounting for Solenoid

Figure 9

FIGURES 10, 11, and 12

Purely elastic distortions of the one, two, three, and four story models with 9 pounds per story when they are vibrating in their natural modes. The elastic displacements are the maxima that will occur when the yield point is just reached in the story indicated by the dotted lines.

The three combinations of yield points assumed for the four story model are:

8, 7, 6 and 5 pounds	Figure 10
8, 6 1/2, 5, and 3 1/2 pounds	Figure 11
8, 6, 4 and 2 pounds	Figure 12

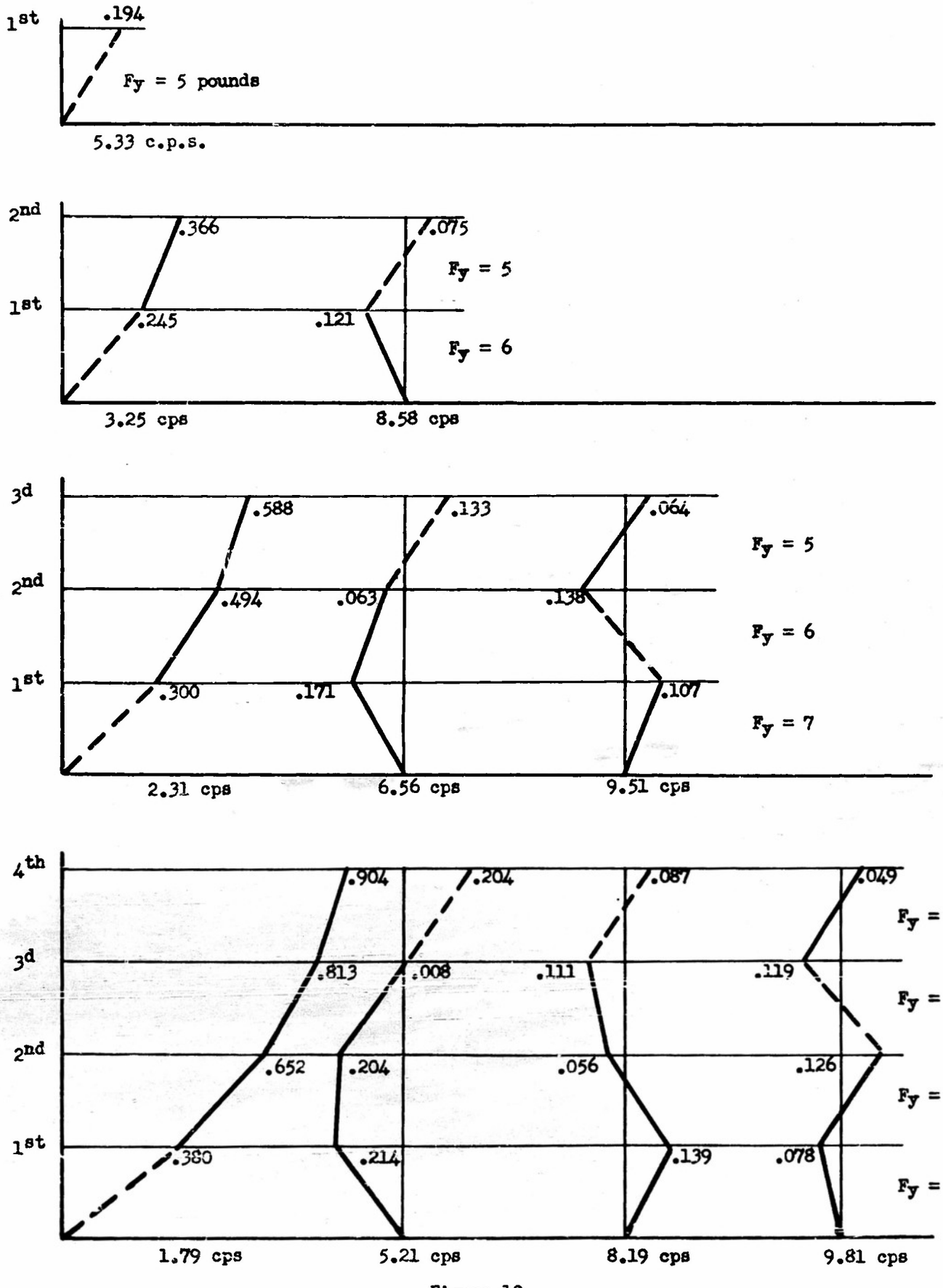

Figure 10

Figure 10

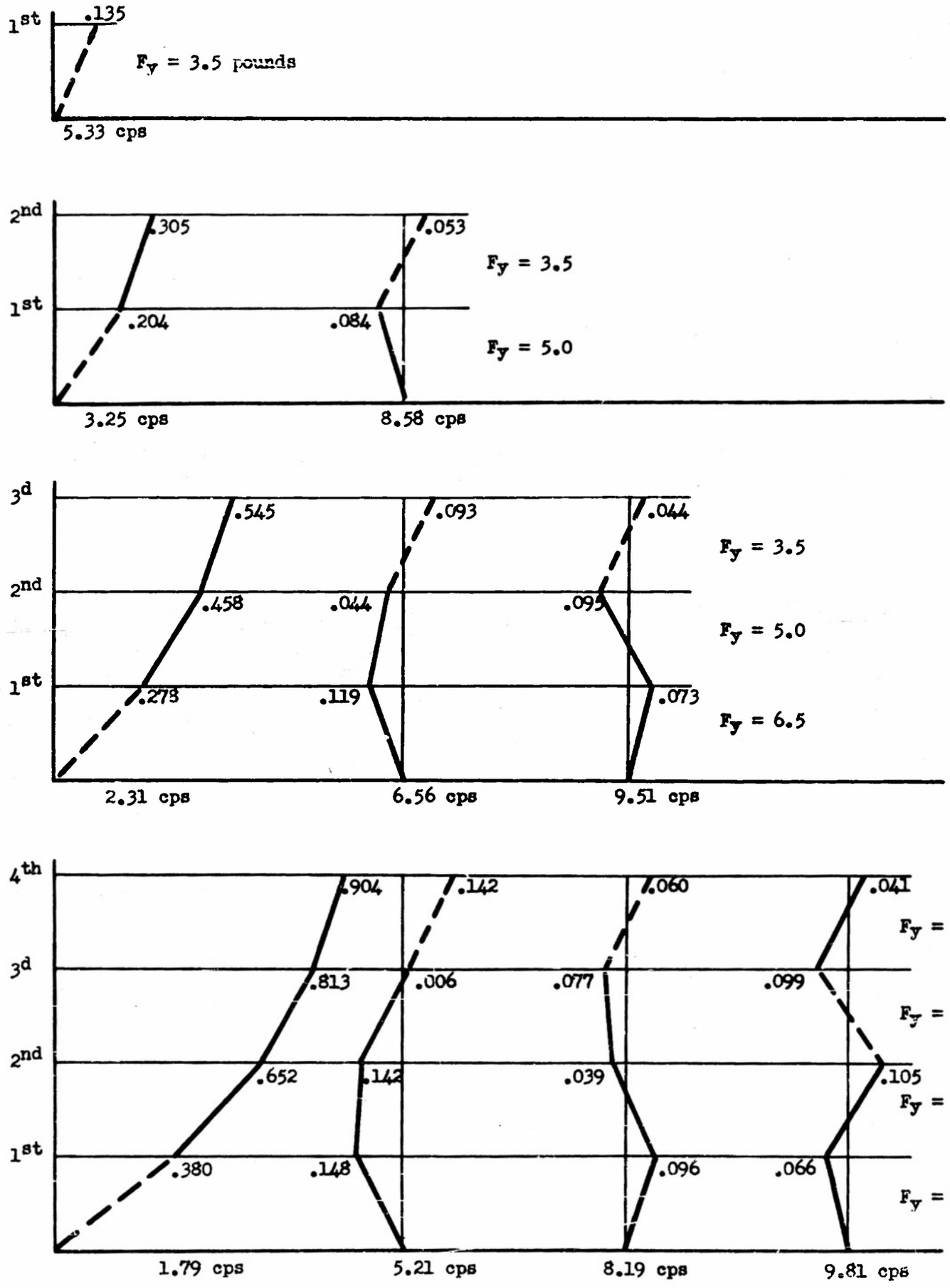

Figure 11

Figure 11

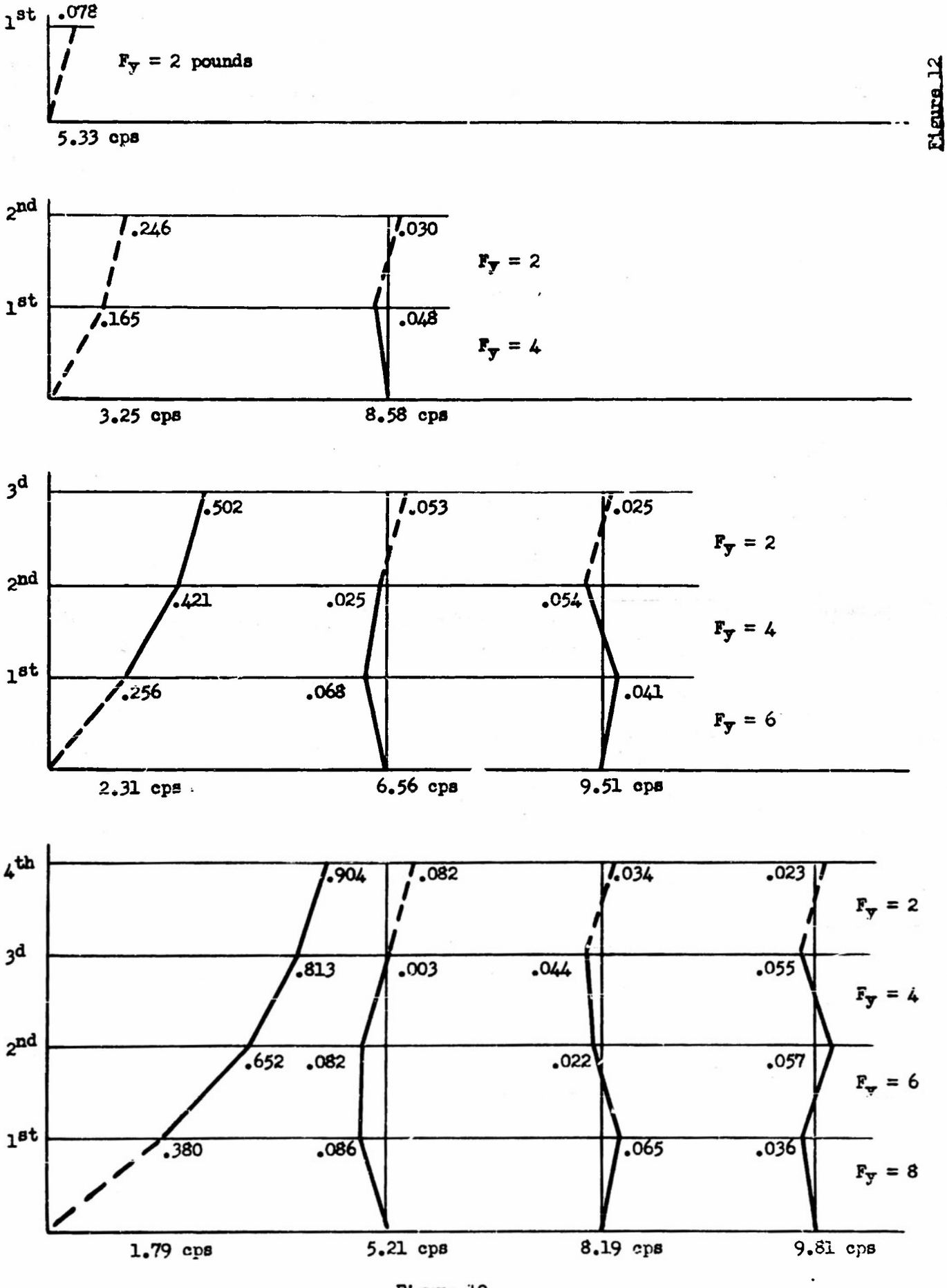

Figure 12

Figure 12

FIGURE 13

The piston force-time relation of the pneumatic loaders used in the tests when they are suddenly exposed to supply pressures and when the supply is suddenly cut off. The maximum rise in pounds per second is approximately 100 times the storage cylinder pressure in pounds per square inch.

In the figure, V_1 is the storage cylinder volume and V_2 is the volume of the loader cylinder plus some piping.

FIGURE 14

The piston force-time relation of the pneumatic loaders when they are suddenly exposed to an air storage of 8 cubic inches at pressures of 20 and 40 psig. The maximum rise in pounds per second is approximately 70 times the storage cylinder pressure in pounds per square inch. Since bleeding occurs past the piston only, the force decreases at a minimum rate. If no bleeding took place, and if the motion of the piston were blocked, the isothermal equilibrium points would be 31 and 15.5 pounds of piston force.

P = 40 and 20 psig; $V_1 = \infty$; V_2 = 2.3 cubic inches
Throttling and Bleeding Minimum

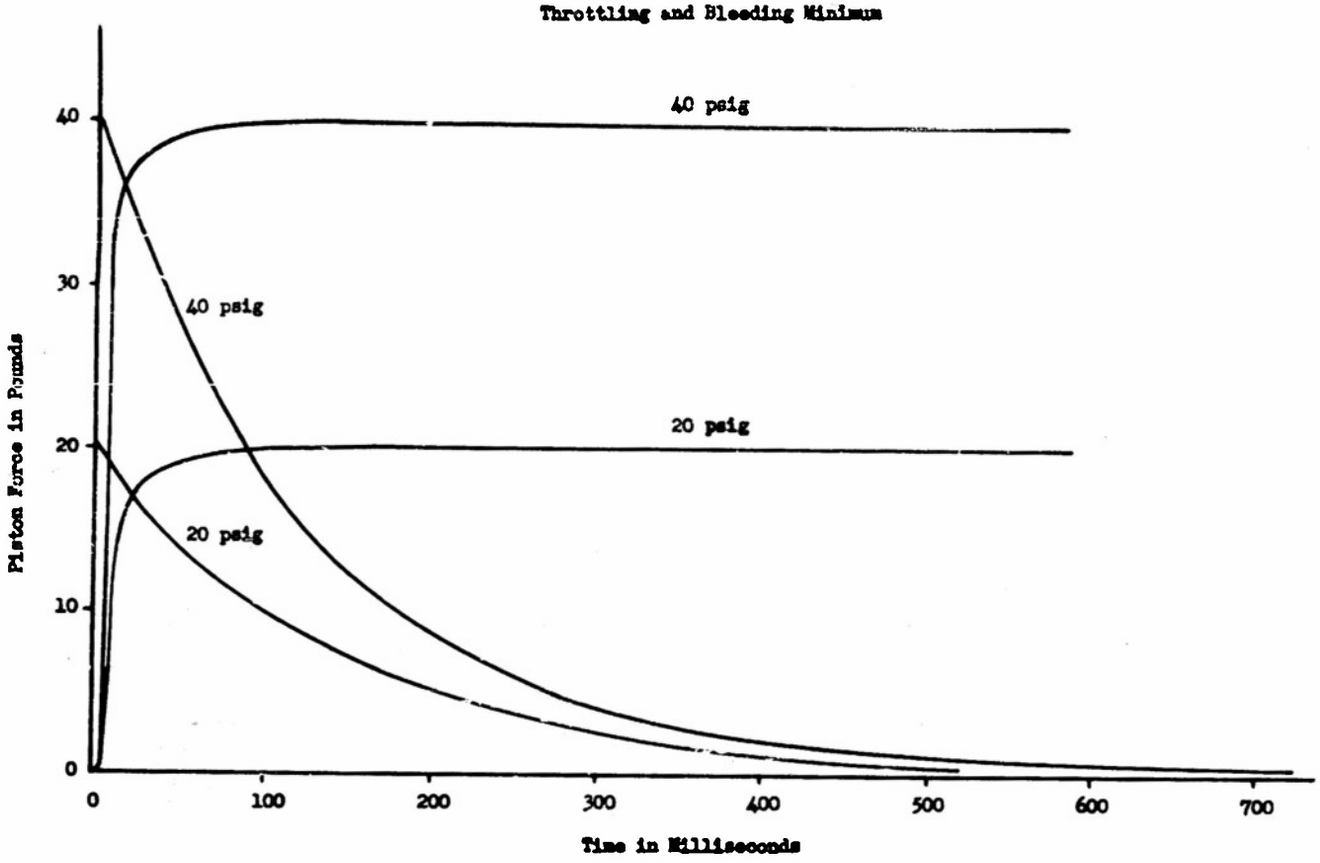

Figure 13

P = 40 and 20 psig; V_1 = 8 cubic inches; V_2 = 2.3 cubic inches
Throttling and Bleeding Minimum

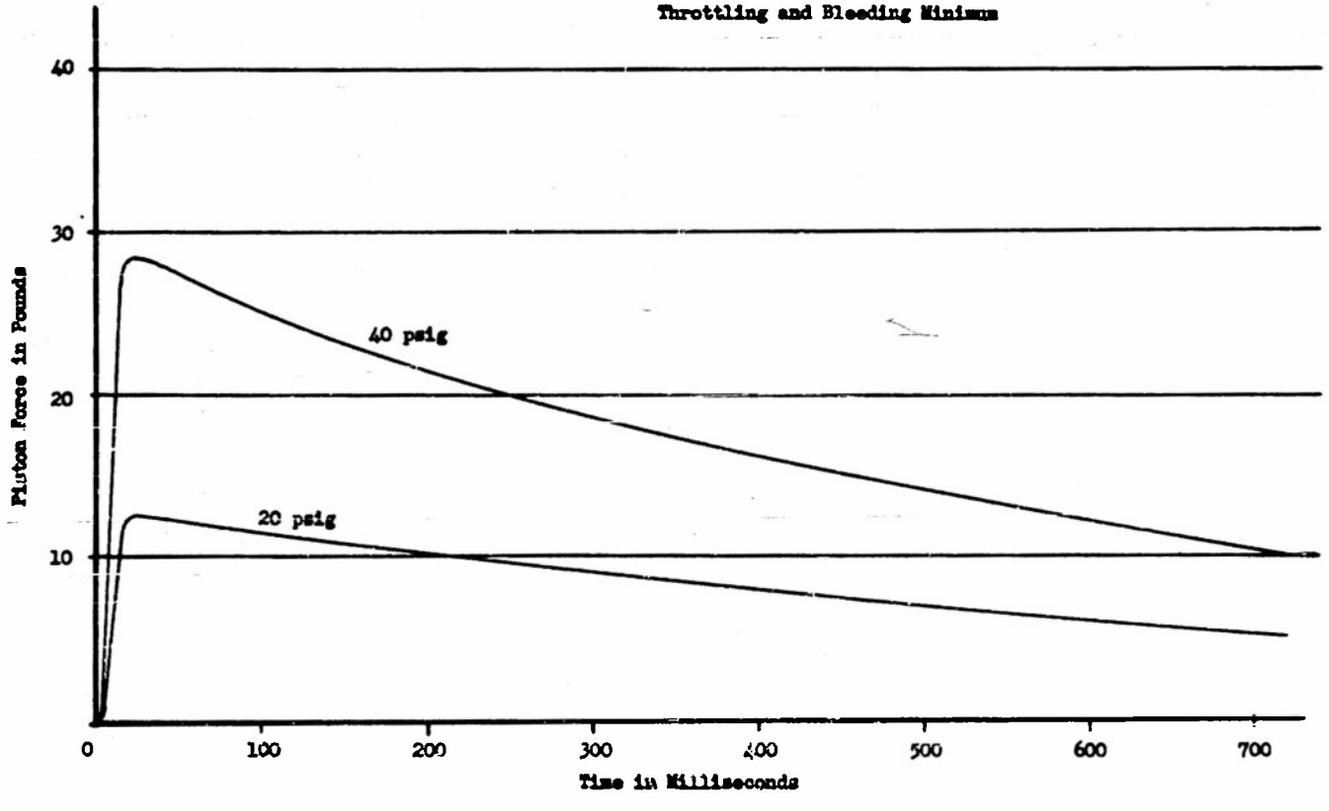

Figure 14

FIGURE 15

The piston force-time relation of the pneumatic loaders when they are suddenly exposed to a volume of 8 cubic inches of air at 20 and 40 psig. As a result of the increased bleeding the maximum piston force is less than in Figure 14, and the force decreases more rapidly than before.

P = 40 and 20 psig; V_1 = 8 cubic inches; V_2 = 2.3 cubic inches

Throttling Minimum, Bleeding 1/2 Turn Open

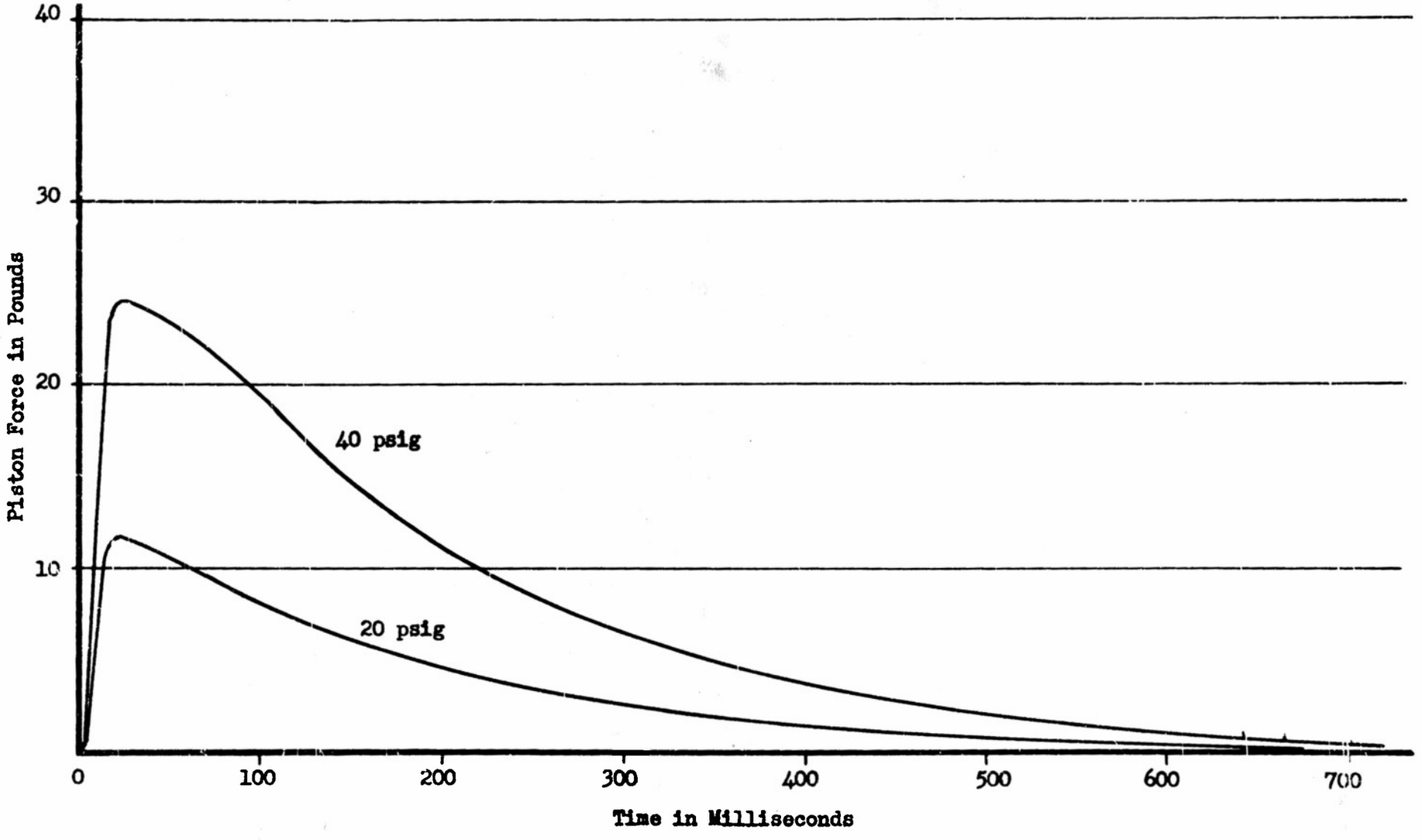

Figure 15

FIGURE 16

The piston force-time relation of the pneumatic loaders when they are suddenly exposed to an air storage of 8 cubic inches at pressures of 20 and 40 psig.

(a) When minimum throttling and maximum bleeding are used.

(b) When the conditions of (a) are modified by a 0.14 pound pop off valve. The peak force F_p is now considerably higher than the maximum force in (a) and the force rise per unit time is also increased. The dotted extensions, cutting the peaks of the curves, define at their upper cut off point a force that we shall call the maximum force F_m as distinguished from the peak force. The reason for recognizing F_m in preference to F_p is that the transient response of the Brush oscillograph system exhibits overshoot in recording the phenomenon when pop-offs are employed.

(c) When the throttle valve is only one half turn open, the force rise per unit time is greatly decreased. This diagram indicates how the time element in the loading may be changed. An increase in air storage volume will have a similar effect.

P = 40 and 20 psig; V_1 = 8 cubic inches, V_2= 2.3 cubic inches

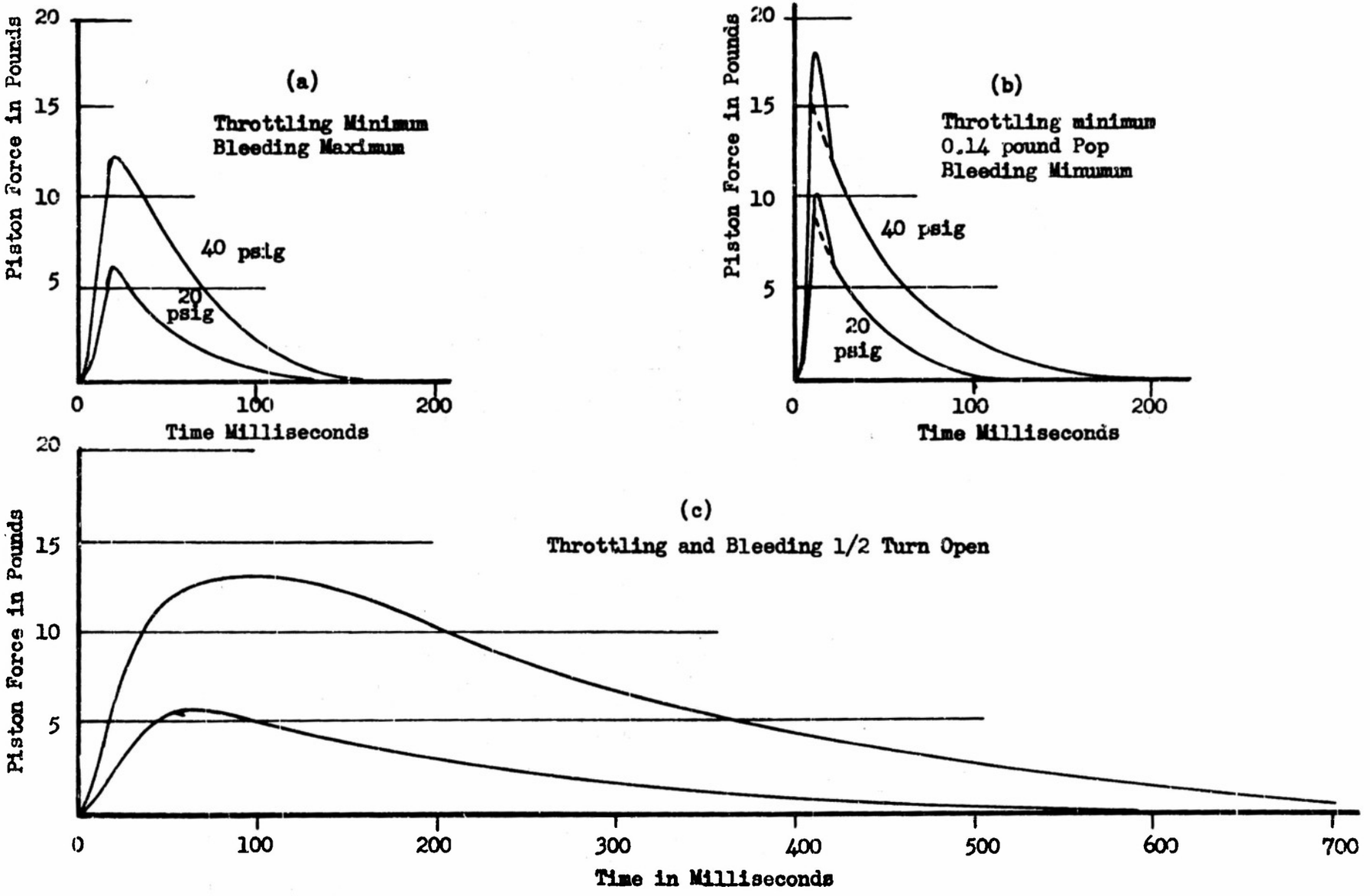

Figure 16

FIGURE 17

The piston force-time relation for the blocked and for the moving single story model as well as the displacement-time record of the moving model. A change in peak force of about 7 percent and a change in impulse of about 10 percent result from the considerable distortion of 2.26 inches. In this case the mass weight of the model was 5.9 pounds, the primary stiffness of the springs was 8.1 pounds per inch and the semi-static brake force F_y was 5 pounds, but the average dynamic brake force F_y' was 7.4 pounds.

The maximum distortional velocity of the motion is seen to be about 30 inches per second and occurs near the time of 30 milliseconds. The average distortion velocity, defined as the maximum displacement M, divided by the time at which it occurs is near 20 inches per second. This average velocity is used in connection with the study of dynamic brake forces, see Figure 36.

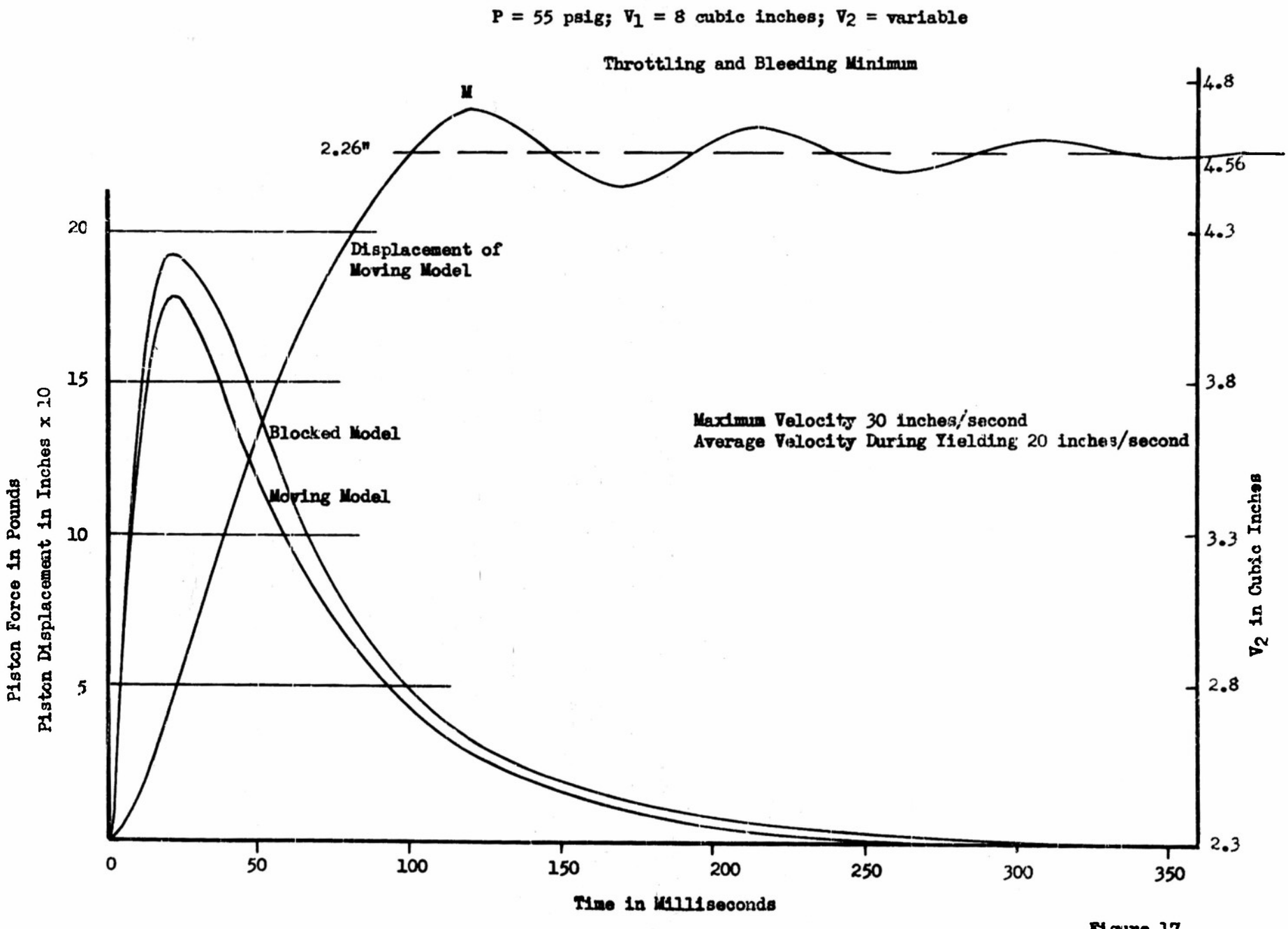
P = 55 psig; V_1 = 8 cubic inches; V_2 = variable
Throttling and Bleeding Minimum
M
2.26"
Displacement of Moving Model
Blocked Model
Moving Model
Maximum Velocity 30 inches/second
Average Velocity During Yielding 20 inches/second
Piston Force in Pounds
Piston Displacement in Inches x 10
V_2 in Cubic Inches
Time in Milliseconds
20
15
10
5
0
50
100
150
200
250
300
350
4.8
4.56
4.3
3.8
3.3
2.8
2.3

Figure 17

FIGURE 18

Piston force-time plots of the four front and four rear loaders (dashed lines) and of the net horizontal force exerted on the model by the four pairs of loaders (full lines). A plot of the roof loader P_5 is shown in solid line. The delays in milliseconds are indicated. These loadings were used for the extensive series of tests described in Figures 20 to 29 inclusive. They are for the horizontal loaders:

Number of Stories	1	2	3	4
Total peak front load, pounds	16.5	33.0	49.5	66.0
Total max. rear load, pounds	0.5	1.8	3.8	6.0
Total front impulse, pound seconds	0.65	1.30	1.95	2.60
Total rear impulse, pound seconds	0.40	0.80	1.20	1.60
Total net horizontal impulse, pound seconds	0.25	0.50	0.75	1.00
Total duration in seconds	0.20	0.21	0.22	0.23

For the roof loader the peak force is 20 pounds; its impulse is 1.25 pound seconds.

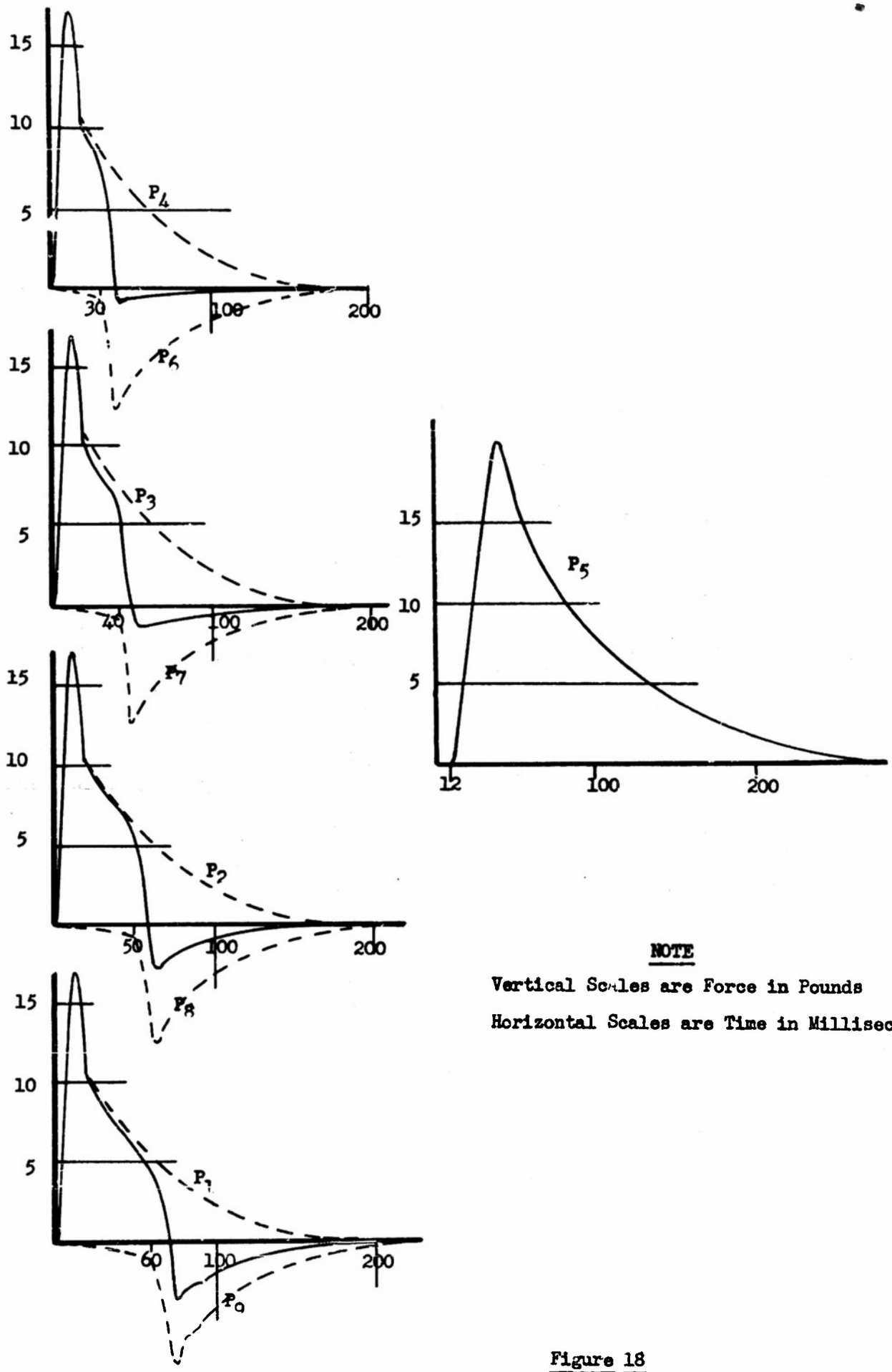

Figure 18

NOTE

Vertical Scales are Force in Pounds

Horizontal Scales are Time in Milliseconds

Figure 18

FIGURE 19

Relationship of piston forces and impulses of loaders with initial pressures in the 8 cubic inch storage cylinders. The larger impulse of the rear loaders is mainly due to their loader cylinder volumes being 7.9 cubic inches (to allow for travel) instead of the 2.3 cubic inches of the front loader cylinders.

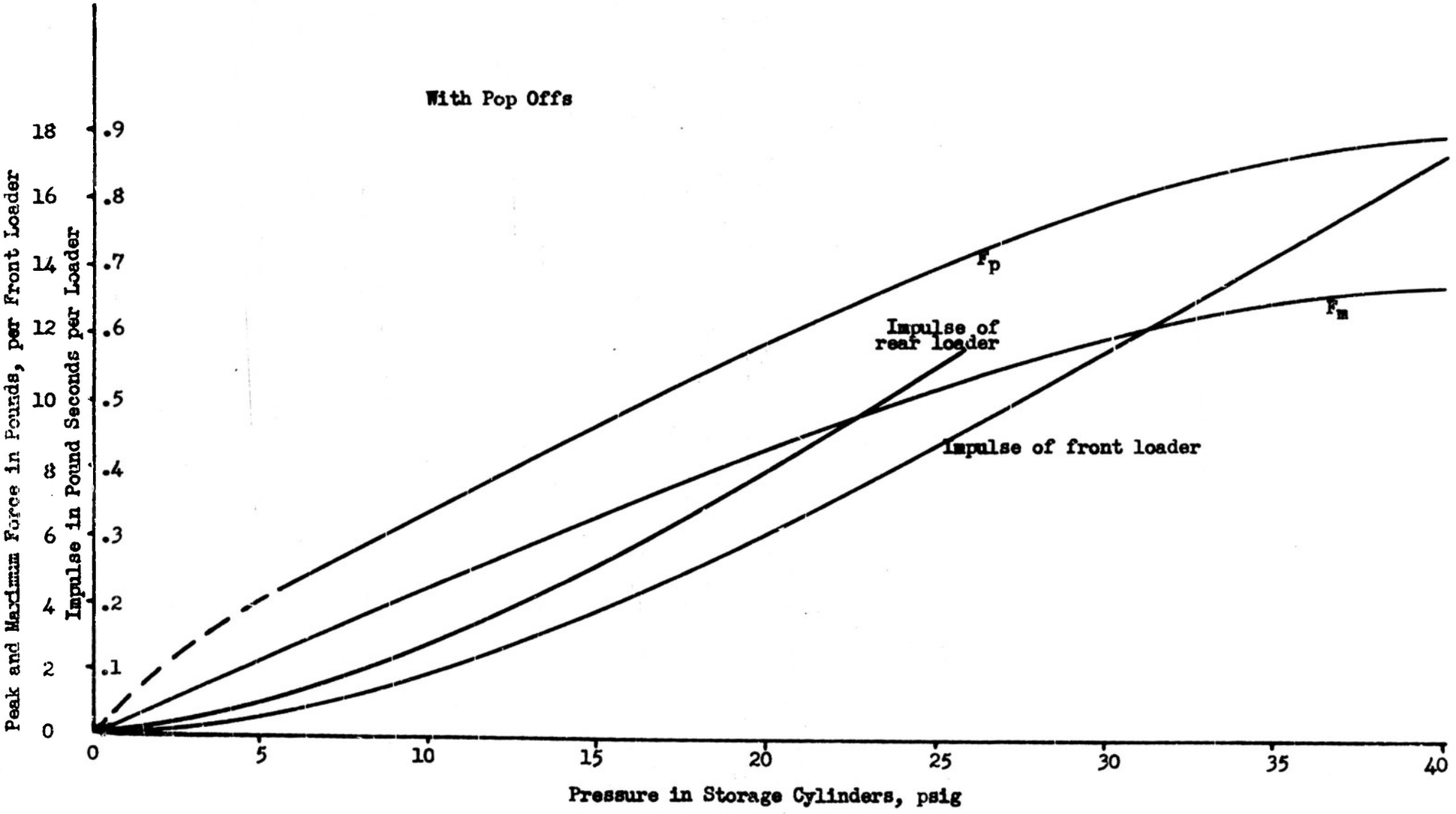
With Pop Offs
Peak and Maximum Force in Pounds, per Front Loader
Impulse in Pound Seconds per Loader
18
16
14
12
10
8
6
4
2
0
.9
.8
.7
.6
.5
.4
.3
.2
.1
F_p
F_m
Impulse of rear loader
Impulse of front loader
0
5
10
15
20
25
30
35
40
Pressure in Storage Cylinders, psig

Figure 19

FIGURES 20 to 29, Inclusive

(9) One story ; F_y = 2; Front and roof loaders only

(14) Two stories ; F_y = 5, 3.5, ; Front loaders only

(14) Two stories ; F_y = 5, 3.5, ; Front and roof loaders only

(20) Three stories ; F_y = 7, 6, 5; Front loaders only

(21) Three stories ; F_y = 7, 6, 5; Front and roof loaders only

(30) Four stories ; F_y = 8, 7, 6, 5; Front and roof loaders only

(32) Four stories ; F_y = 8, 6.5, 5, 3.5; Front loaders only

(36) Four stories ; F_y = 8, 6, 4, 2; Front and roof loaders only

Only one collapse in stories other than the first took place; see diagram (36) Fig. 29 where the second story with F_y = 6 pounds proved to be the weakest of the four stories.

Note that the dynamic brake forces F_y' are variable and larger than the semi-static ones used in the tests. See Figures 35 and 36.

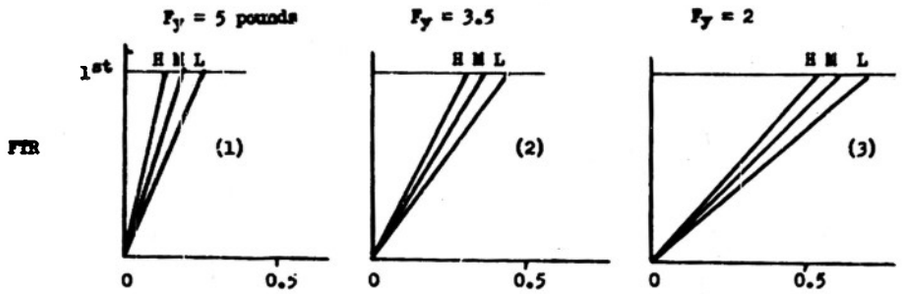

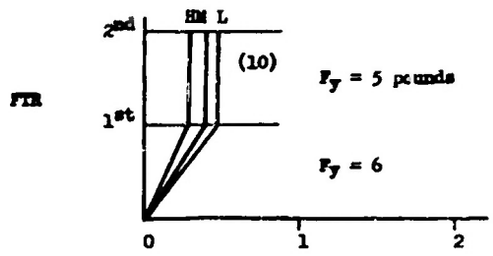

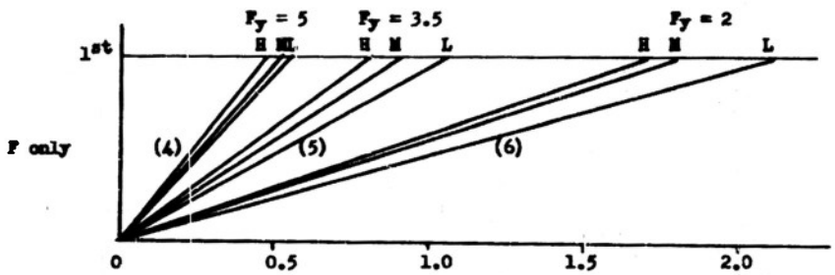

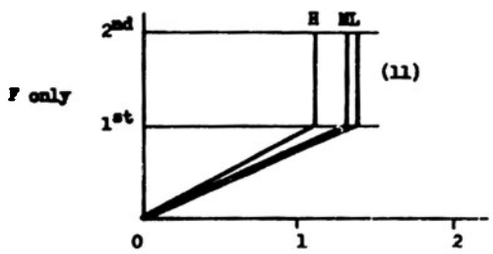

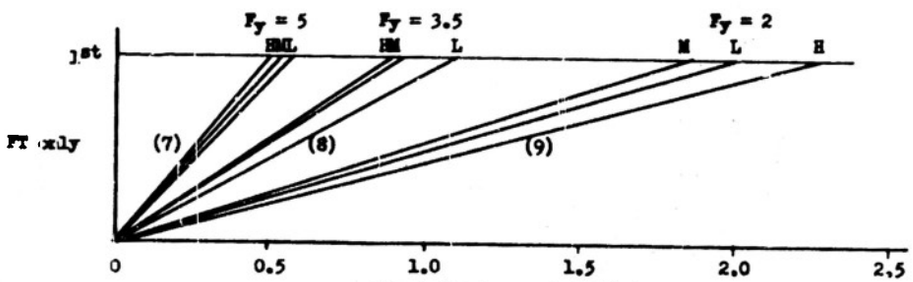

Figure 20

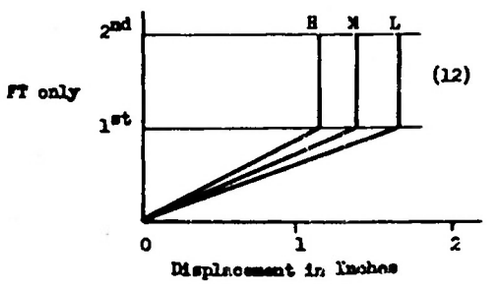

Figure 21

FIGURES 20 to 29, inclusive (diagrams 1 to 36)

Final displacement curves of the one, two, three, and four story model produced by the loadings described in Figure 18. The three combinations of yield forces F_y given in Figures 10, 11, and 12 have been used, and the symbols L, M, H refer to the light, the medium, and the heavy story weights of 9, 12, and 15 pounds respectively.

Three load combinations have been used, namely: all loaders (FTR), front loaders (F) only, and front and roof loaders (FT) only.

No collapses resulted when all loaders were used. When collapses occurred, usually in the bottom story, the model was caught by hand so as not to disturb the distortions in the non-collapsing stories. An experimental determination of the maximum static deflection at which the story in question would just collapse was then made. This determination agreed in all cases with the calculated value within plus or minus 9 percent. However, in plotting curves the calculated maximum static distortions producing collapse have been used. Collapse is indicated by the dotted lines.

In general the L-model composed of 9 pound stories shows greater distortions that the M-model of 12 pound stories, and the 15 pound H-model suffers the least; but if collapse is imminent so that the vertical load becomes important, the sequence L M H is not always maintained. Sequence irregularities occur in the following diagrams:

Cont'd

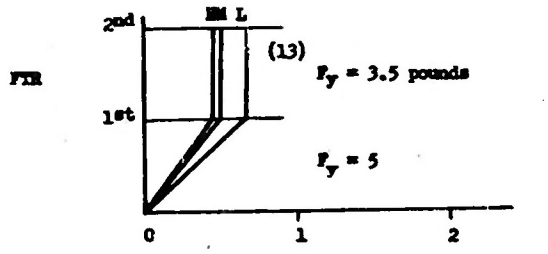

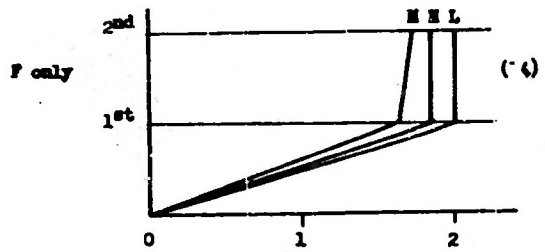

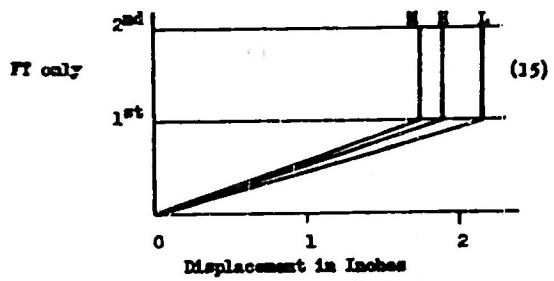

Figure 22

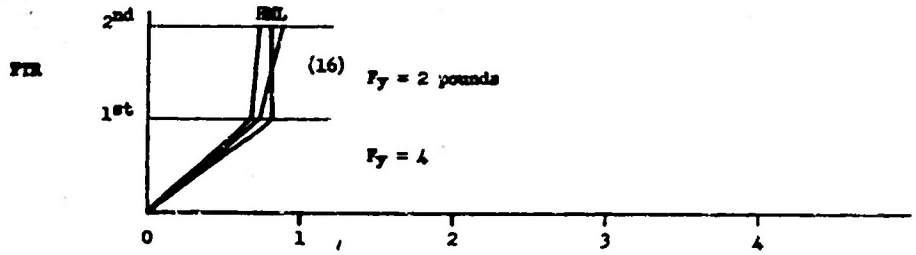

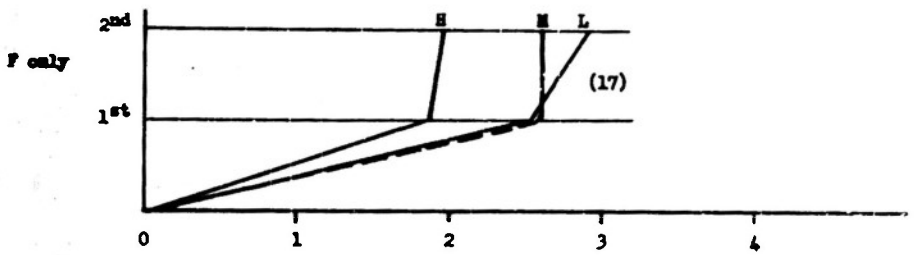

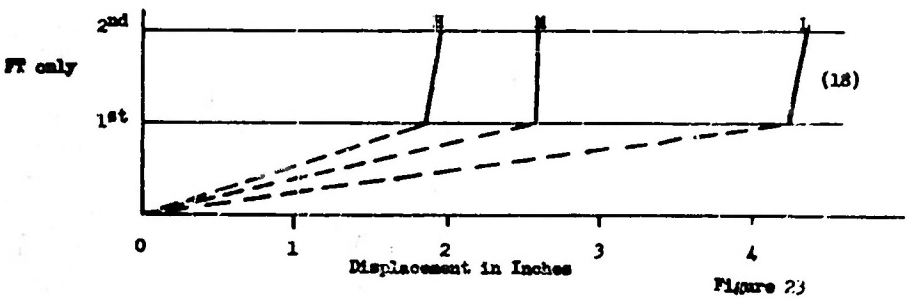

Figure 23

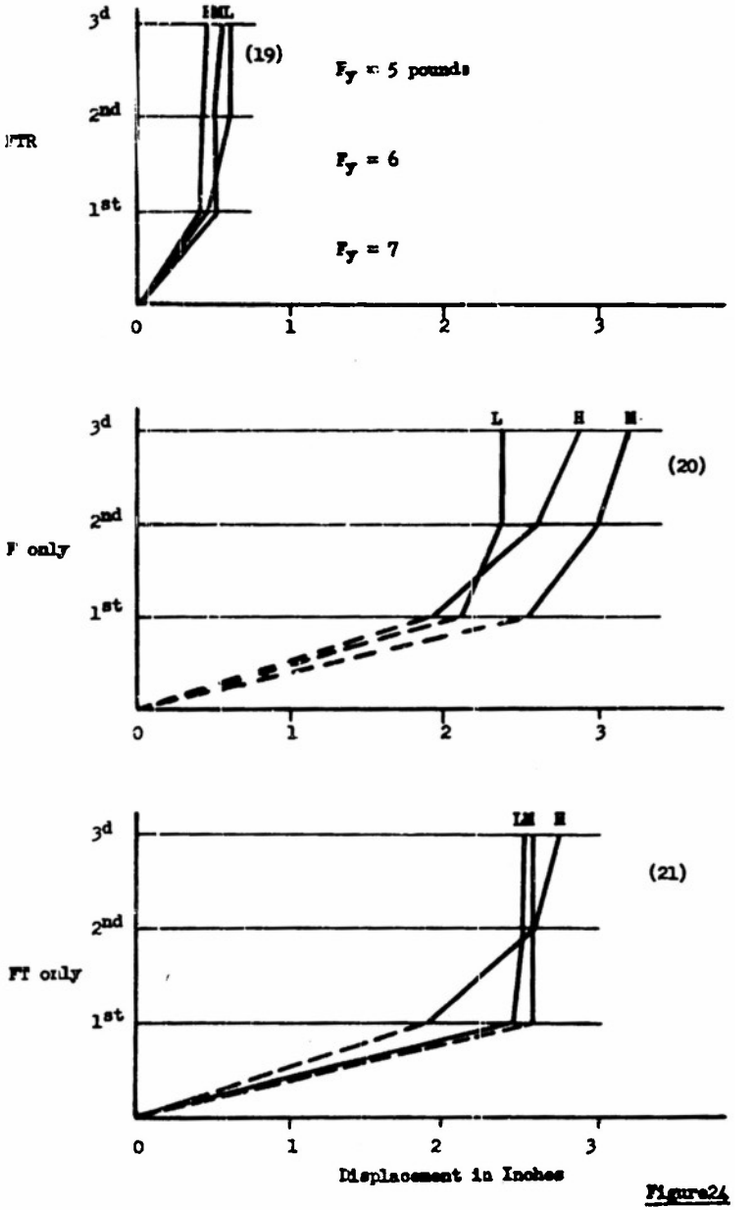

Figure24

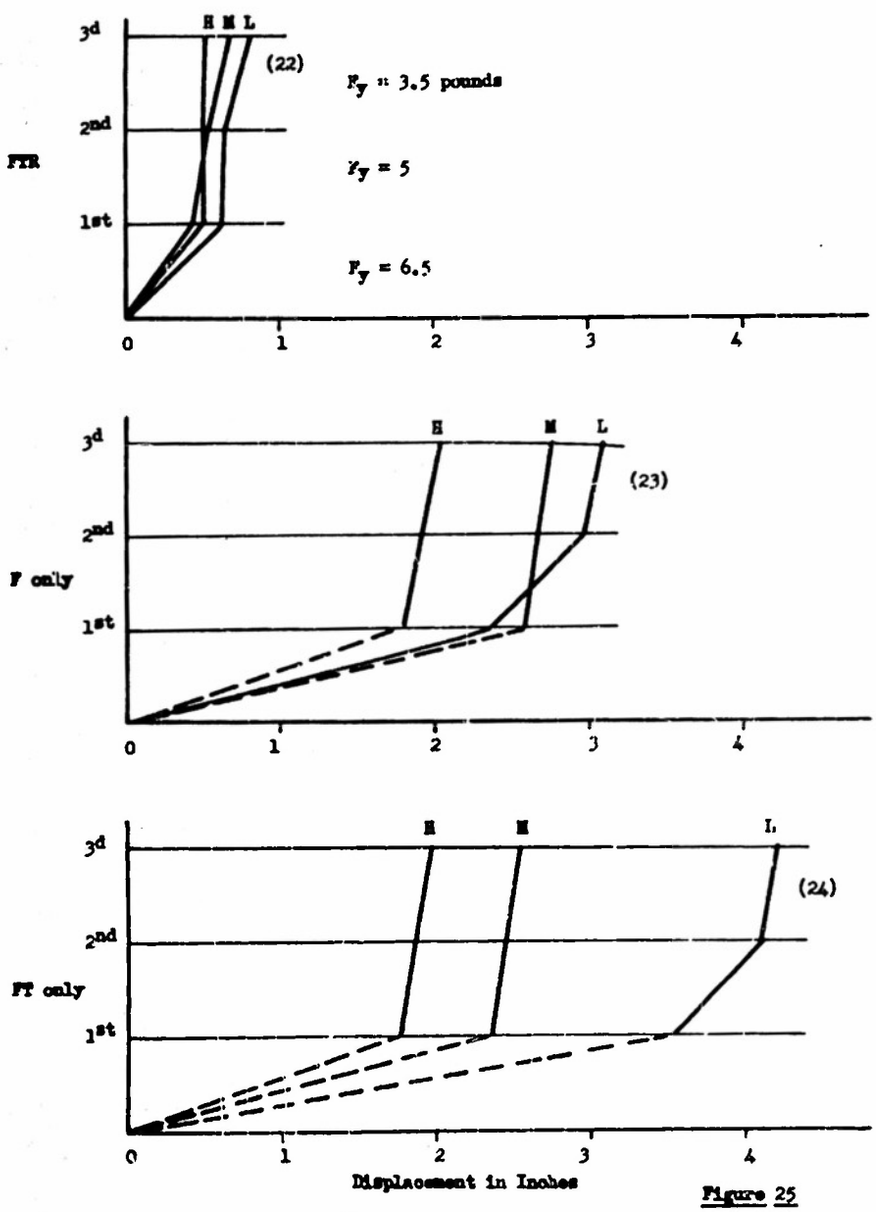

Figure 25

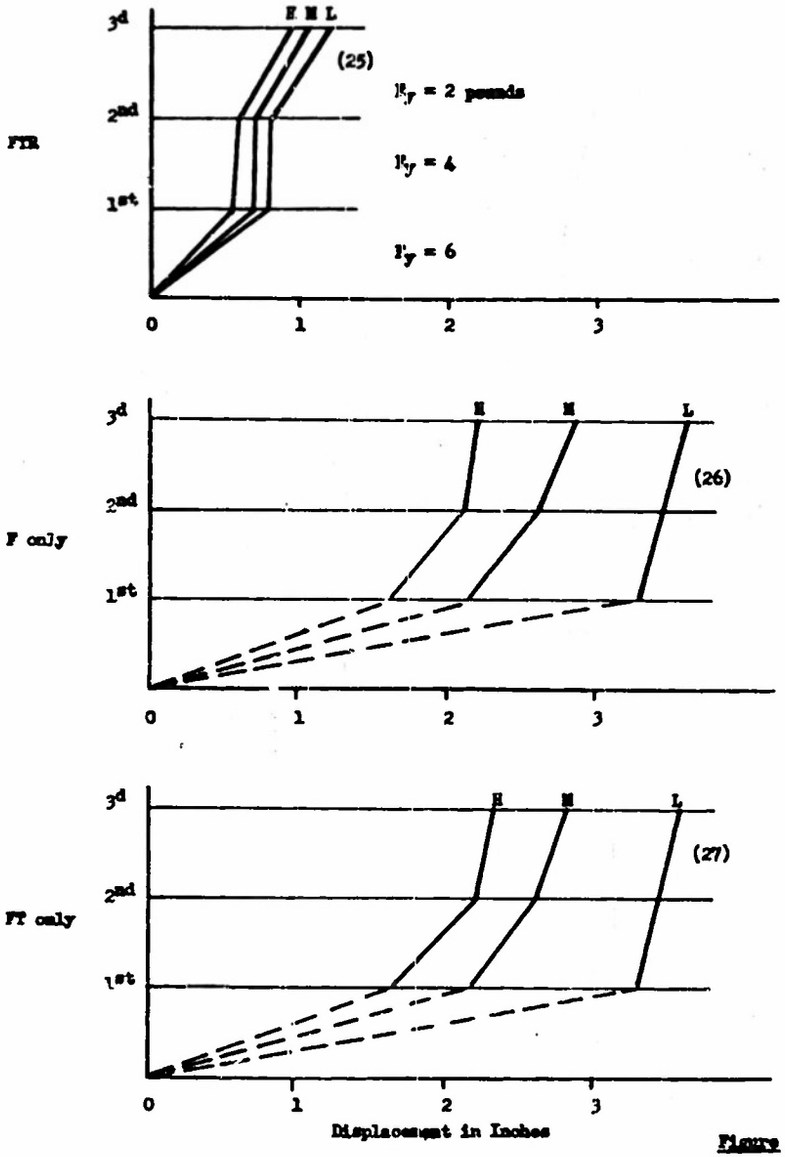

Figure 26

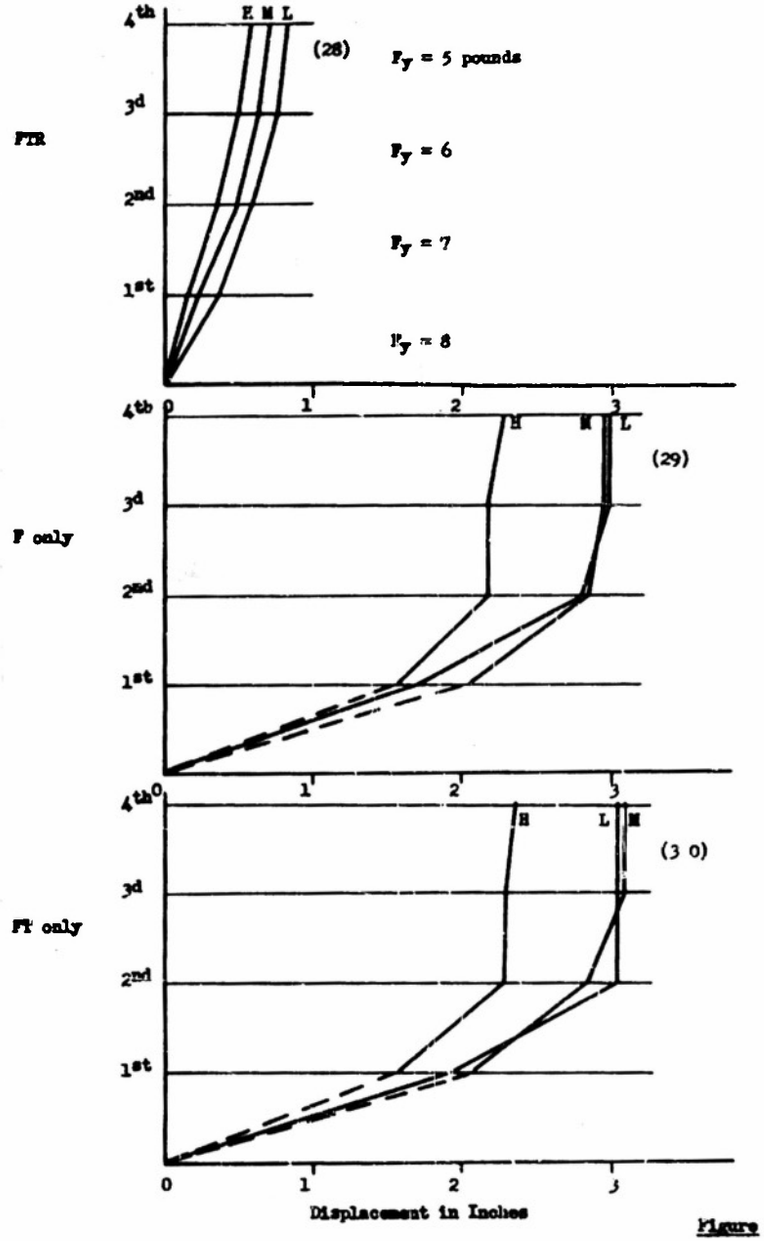

Figure 27

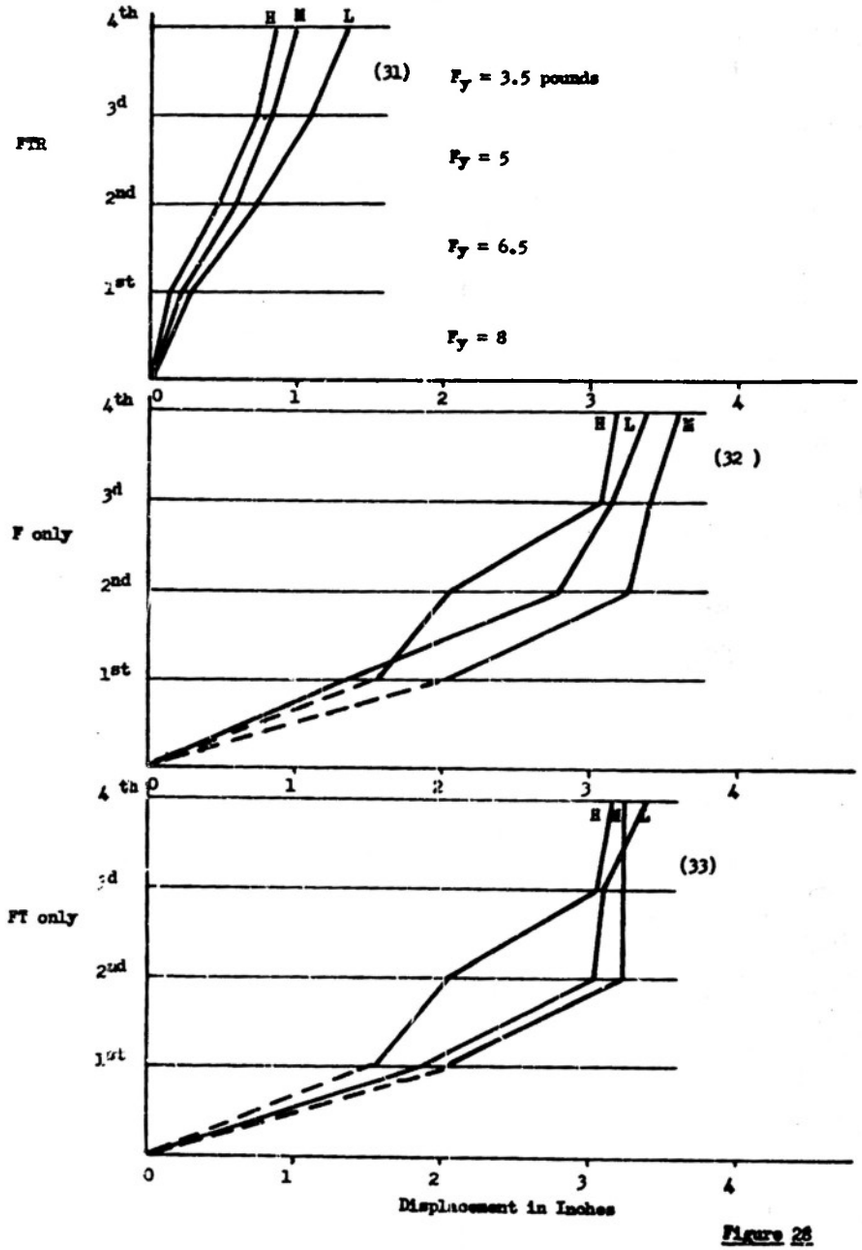

Figure 28

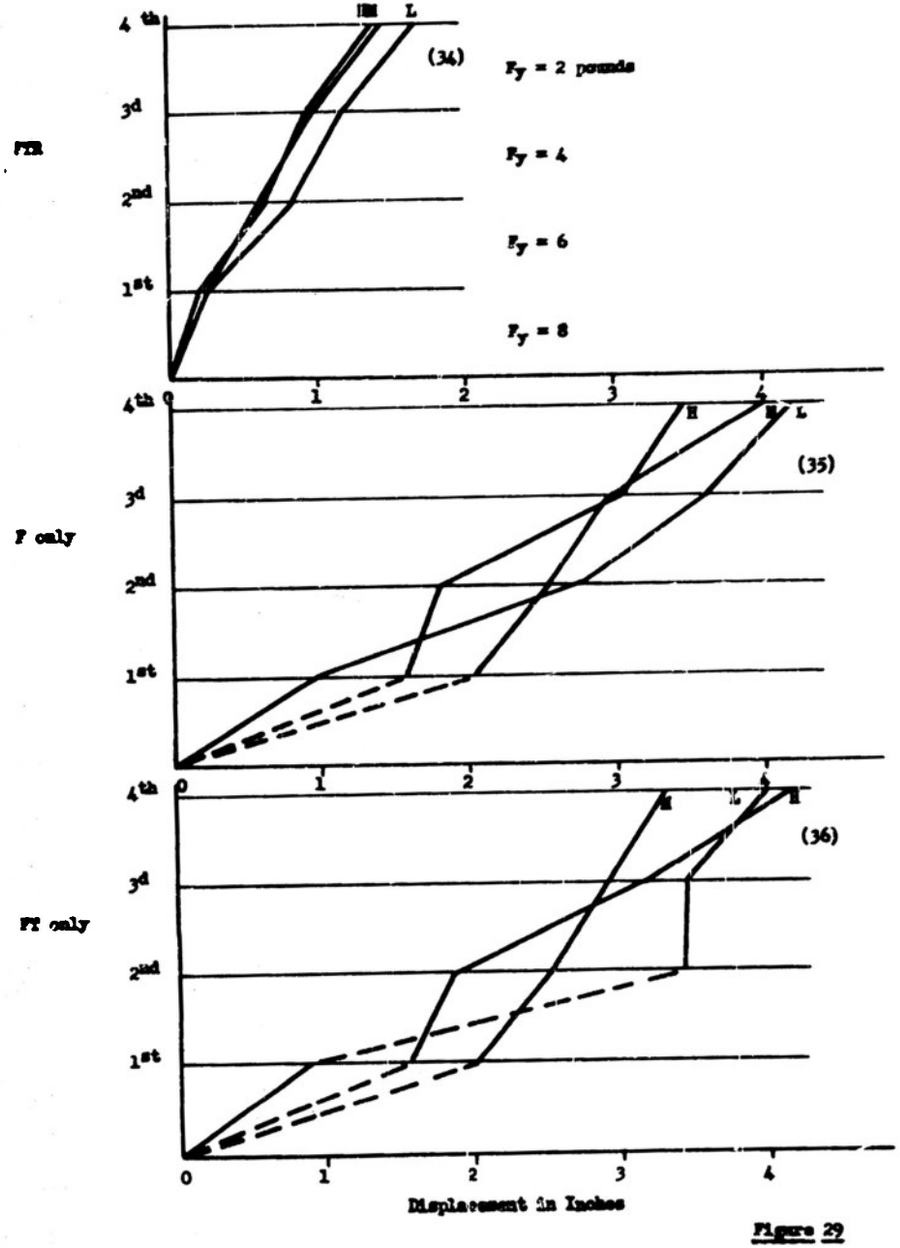

Figure 29

FIGURE 30

Loader forces and final displacement of the one story model plotted against loader impulse. It is seen that for an impulse smaller than about 0.08 pound seconds the model suffers only elastic displacements. The single story model with a semi-static brake force $F_y = 5$ pounds and with K_p equal to 1.7 pounds per inch cannot be collapsed by the maximum forces obtainable from the model's loaders. Note that the dynamic brake force F_y' is not constant. See Figures 35 and 36.

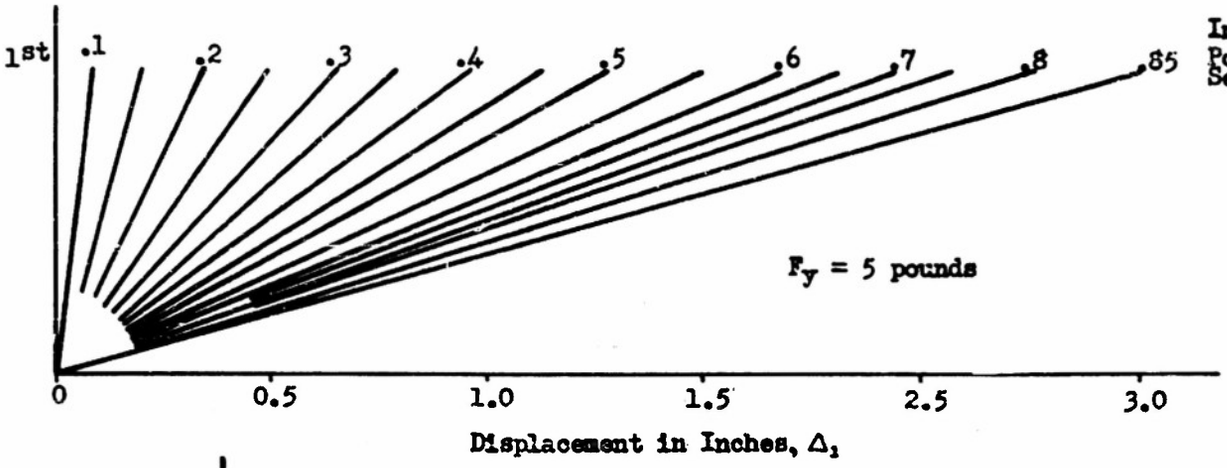

Figure 20

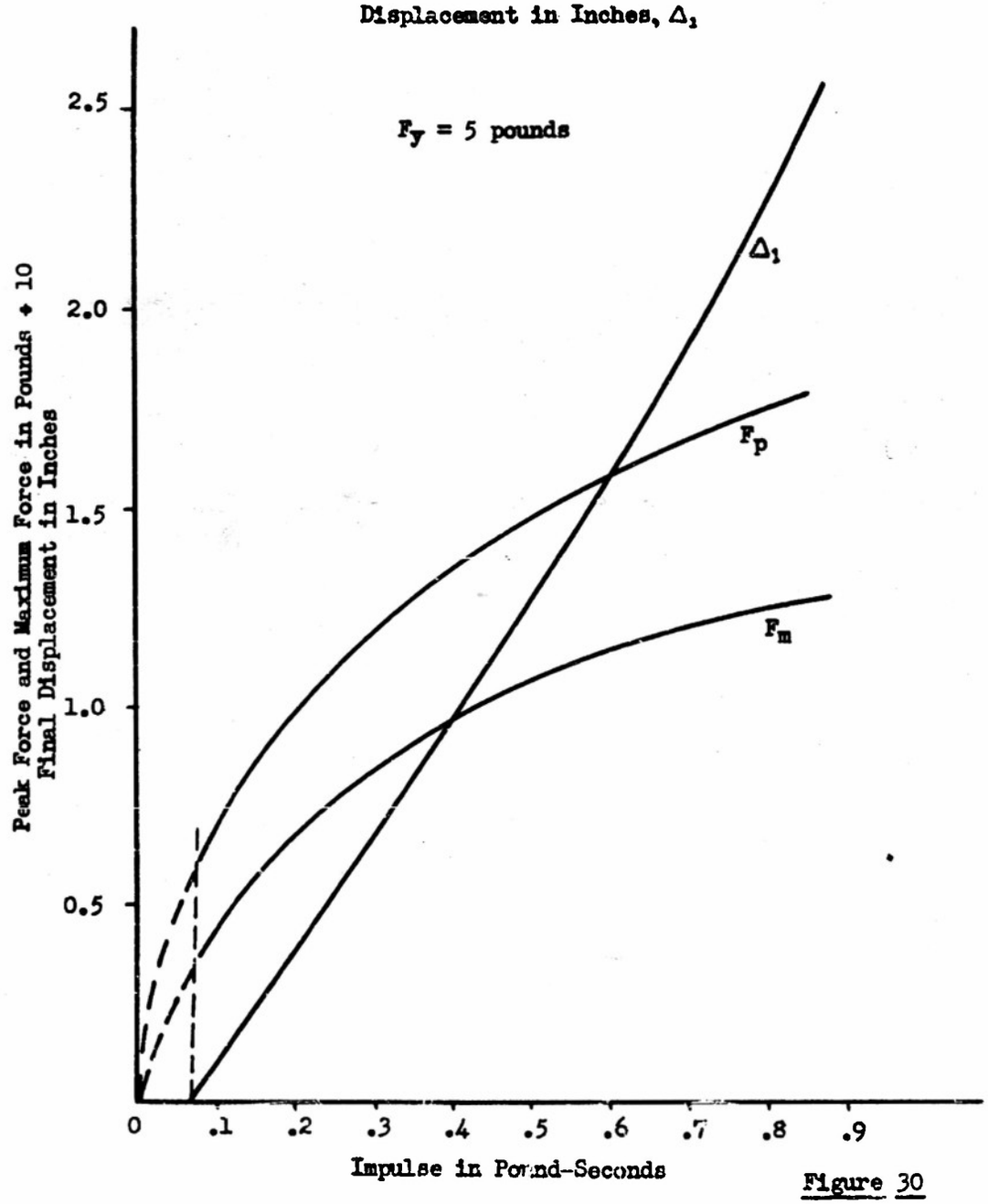

Figure 30

FIGURE 31

Displacements of the four story model plotted for constant increments in front loader total impulse up to collapse of the bottom story. The semi-static values of F_y were 8, 7, 6, and 5 pounds for stories 1 to 4, respectively

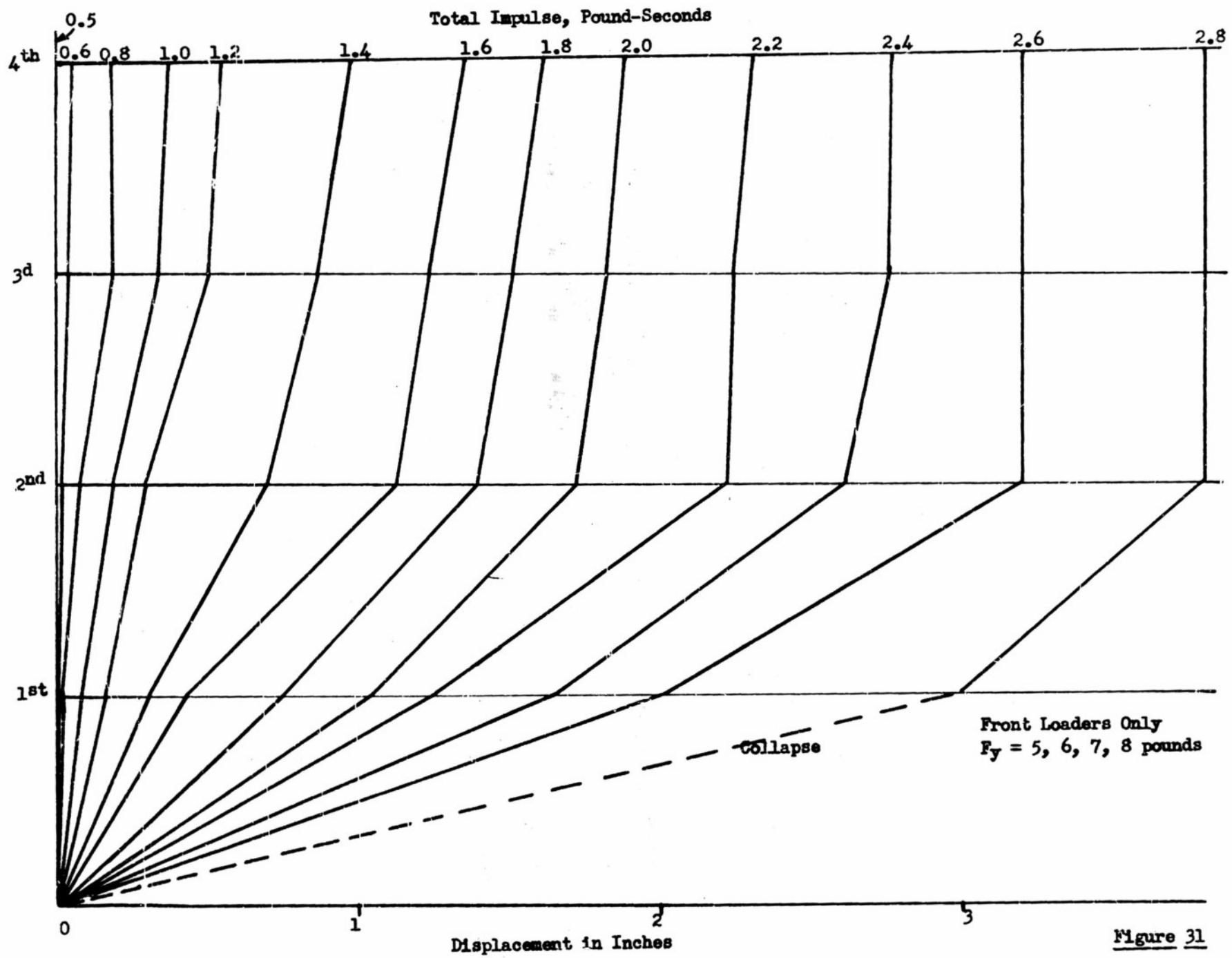
Total Impulse, Pound-Seconds
0.5
0.6
0.8
1.0
1.2
1.4
1.6
1.8
2.0
2.2
2.4
2.6
2.8
4th
3d
2nd
1st
Collapse
Front Loaders Only
Fy = 5, 6, 7, 8 pounds
0
1
2
3
Displacement in Inches

Figure 31

FIGURE 32

A plot of piston forces, final distortions of each story, final top displacement, and plastic work against total loader impulse up to the point of collapse. Near the collapsing load Δ_1, Δ_4, and the plastic work increase very rapidly.

It is seen that the four story model with F_y = 8, 7, 6, and 5 pounds will not suffer plastic distortions until the total impulse exceeds 0.5 pound inches. This is about a 67 percent higher impulse tolerance for its elastic behavior than that of the one story model.

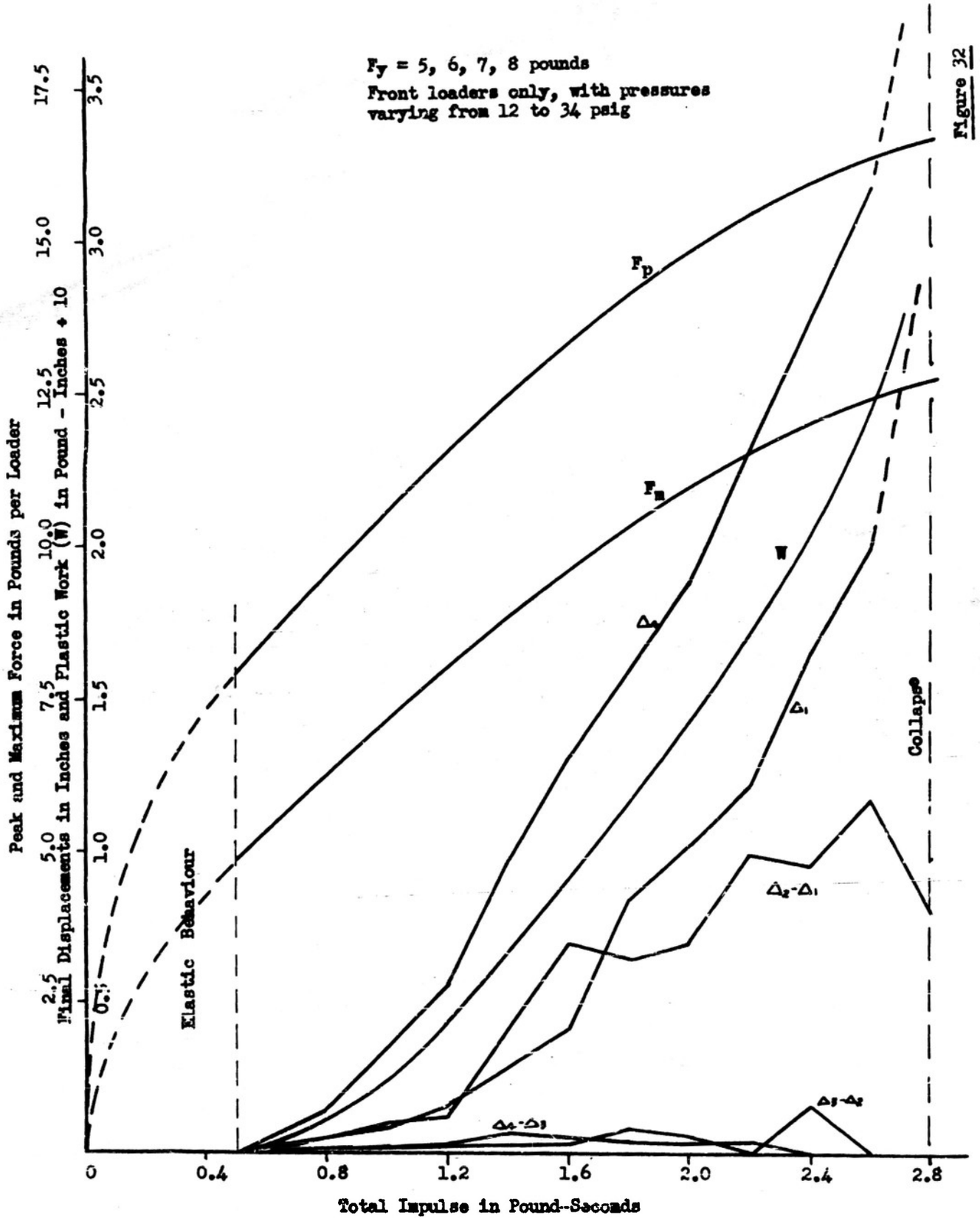
F_y = 5, 6, 7, 8 pounds
Front loaders only, with pressures varying from 12 to 34 psig
Figure 32
Peak and Maximum Force in Pounds per Loader
Final Displacements in Inches and Plastic Work (W) in Pound - Inches ÷ 10
F_p
F_m
W
Δ_4
Δ_1
$\Delta_2-\Delta_1$
$\Delta_3-\Delta_2$
$\Delta_4-\Delta_3$
Elastic Behaviour
Collapse
Total Impulse in Pound-Seconds
0
0.4
0.8
1.2
1.6
2.0
2.4
2.8
2.5
5.0
7.5
10.0
12.5
15.0
17.5
1.0
1.5
2.0
2.5
3.0
3.5

Figure 32

FIGURE 33

Displacements of the four story model plotted for constant increments in front loader total force up to collapse of the bottom story. The semi-static values of F_y were 8, 7, 6, and 5 pounds respectively. Non-linearity of displacement and force is apparent.

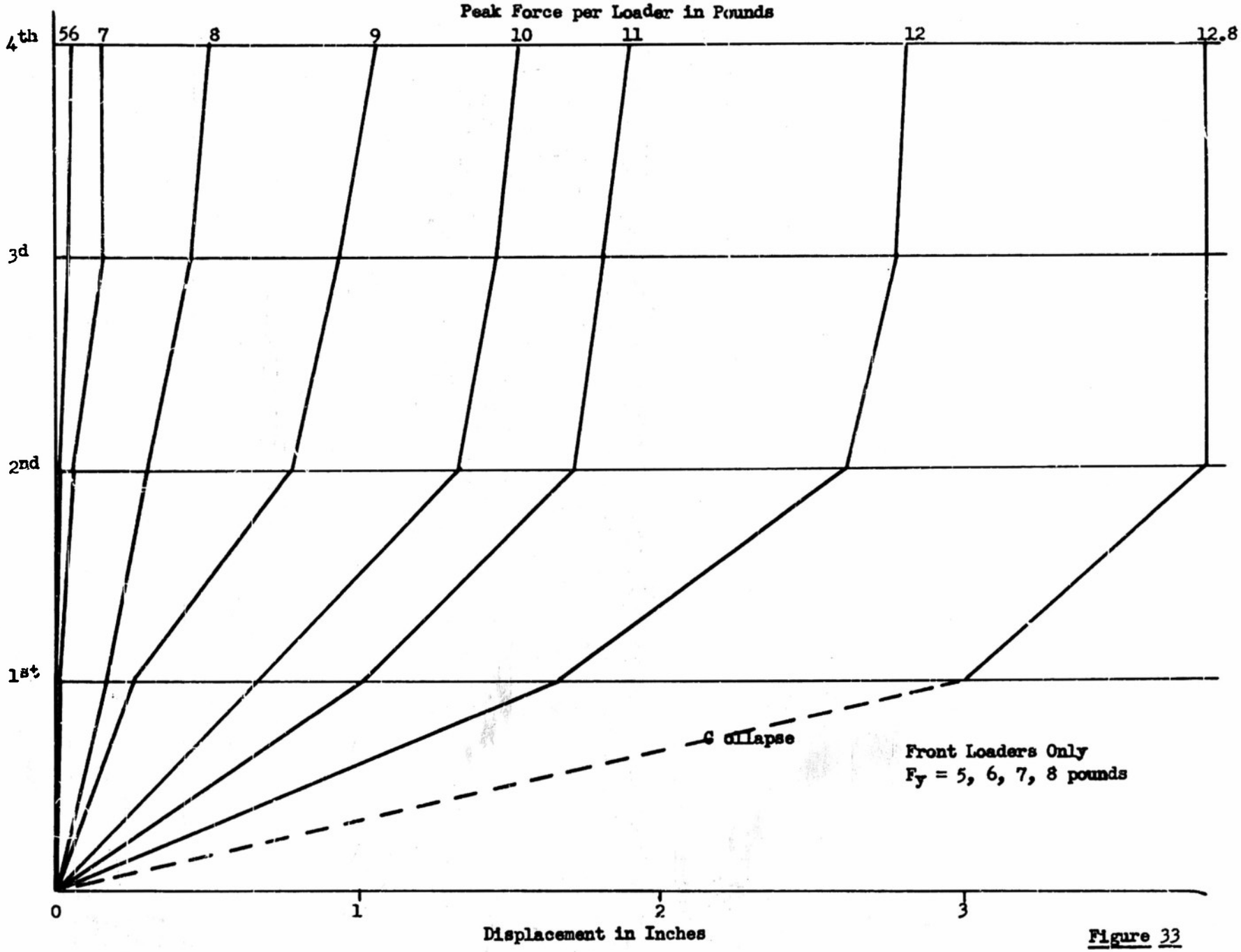
Peak Force per Loader in Pounds
4th
3d
2nd
1st
5 6 7 8 9 10 11 12 12.8
0 1 2 3
Displacement in Inches
Collapse
Front Loaders Only
Fy = 5, 6, 7, 8 pounds

Figure 33

FIGURE 34

Displacements of the four story model under the simultaneous action of the front loaders, followed, after a time delay of t seconds, by the simultaneous action of the rear loaders.

The total positive impulse of 2.60 pound seconds is followed t seconds later by a negative impulse of 1.60 pound seconds making the net impulse 1.00 pound inches for all the time marked curves. As a comparison, the curves corresponding to a front loader only application of 2.60 pound inches impulse, and the collapsing curve for a 2.80 pound second impulse are shown.

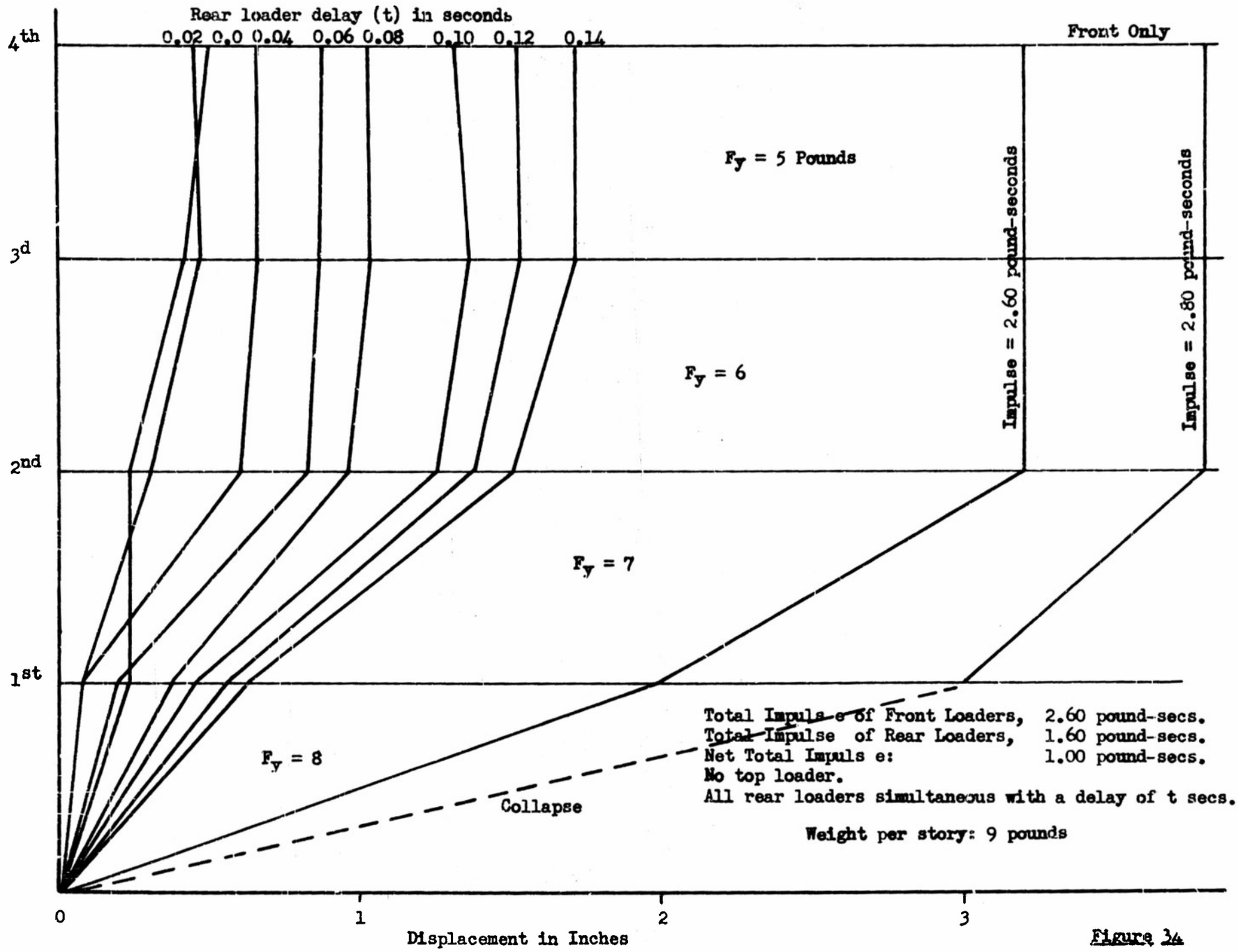
Rear loader delay (t) in seconds
0.02 0.0 0.04 0.06 0.08 0.10 0.12 0.14
Front Only
4th
3d
2nd
1st
F_y = 5 Pounds
F_y = 6
F_y = 7
F_y = 8
Impulse = 2.60 pound-seconds
Impulse = 2.80 pound-seconds
Collapse
Total Impulse of Front Loaders, 2.60 pound-secs.
Total Impulse of Rear Loaders, 1.60 pound-secs.
Net Total Impulse: 1.00 pound-secs.
No top loader.
All rear loaders simultaneous with a delay of t secs.
Weight per story: 9 pounds
0
1
2
3
Displacement in Inches

Figure 34

FIGURE 35

Average dynamic braking force F_y' plotted against final distortion of the one story model.

In this case the semi-static braking forces, F_y, were set experimentally at 5, 8, and 10 pounds by observing the dynamic records of the S. R. 4 gauges on the flat leaf springs used as primary restoring elements (Figure 7). The front loader forces were then increased to produce the final distortion dynamically. Simultaneous records of primary spring force, loader force, model distortions, and model velocity were taken.

The empriical relation, involving the final distortion Δ as the independent variable,

$$F_y' = F_y(1 + 0.04\ F_y\Delta),$$

where F_y, and F_y' are in pounds and Δ is in inches gives a reasonable fit, showing that considerable changes with Δ will occur in the average dynamic braking force. The above relation may, be used for "estimating" the dynamic brake force F_y'.

FIGURE 36

The average dynamic braking force, F_y', plotted against the average distortional velocity, V_a, of the one story model.

The average distortional velocity is specifically indicated in Figure 17; it is approximately equal to the average velocity (V_a) of the "plastic" distortion. The empirical relation

$$F_y' = F_y(1 + 0.0015\ V_a^2),$$

where F_y, F_y' are in pounds and V_a is in feet per second, has been plotted. This relation may be used in correlating an "estimate" of the dynamic brake force F_y' with experimental data relating to the dynamic loading of frame structures.

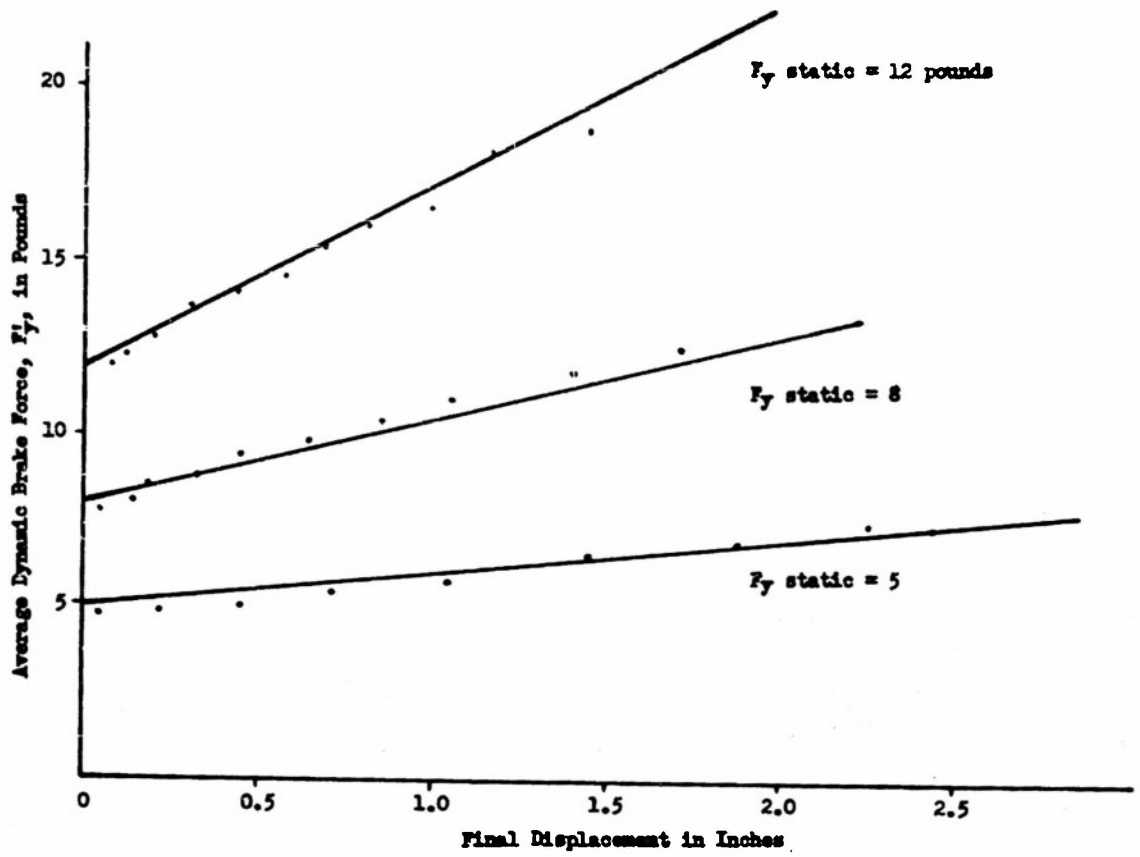

Figure 35

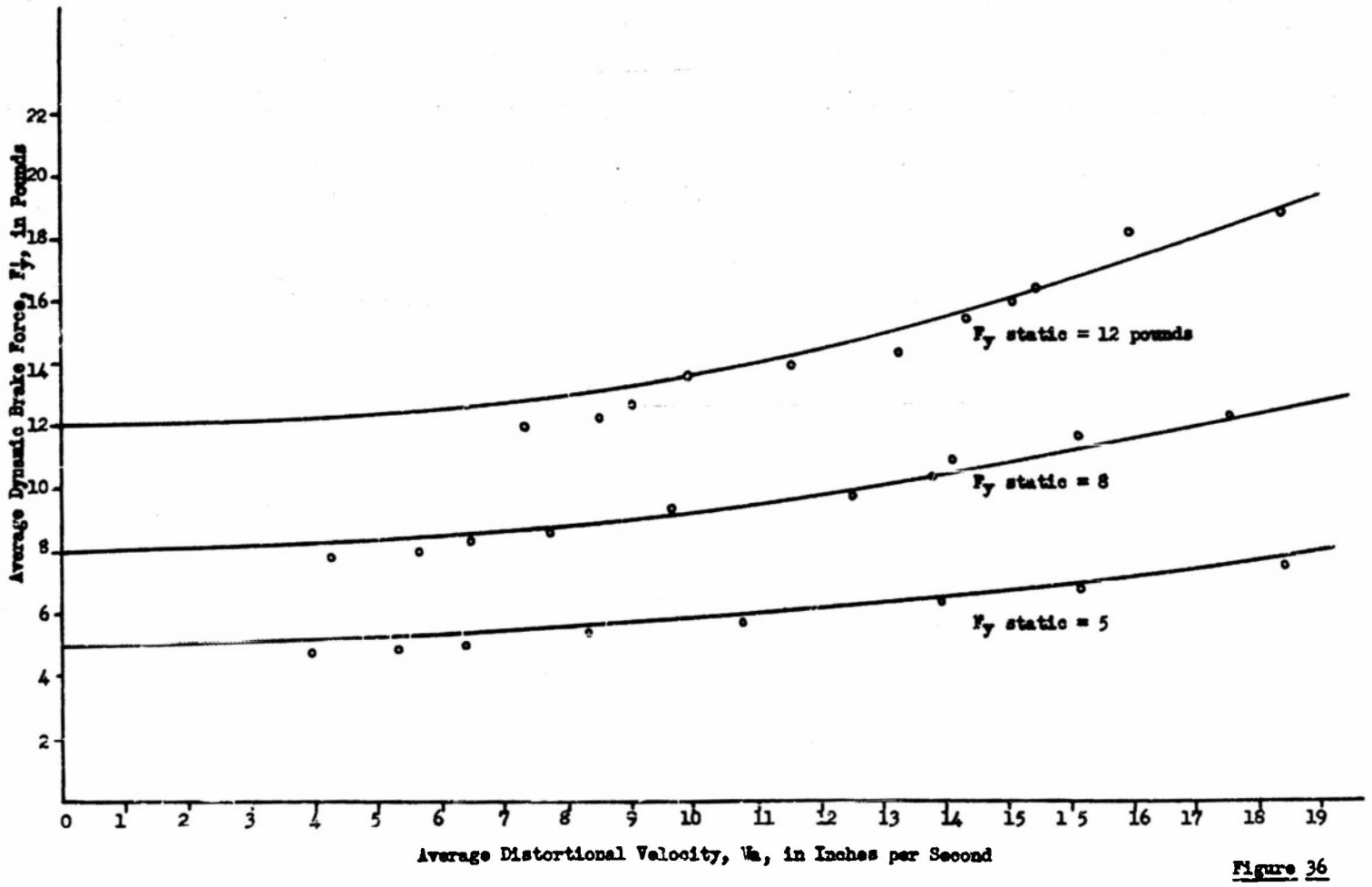

Figure 36

FIGURE 37

Experimental data relating the maximum front loader force and impulse with gauge pressure in the 8 cubic inch storage cylinder. The data in this plot is used in Figure 38.

FIGURE 38

Final displacement of a one story model with average dynamic loading forces held at constant values by successive experimental approximations. Impulse found from Figure 37 is taken as the independent variable.

The model with $F_y' = 2$ pounds collapses when the impulse is about 0.47 pound seconds. With $F_y' = 5$ pounds, it requires an impulse of 1.08 pound inches before collapse occurs or 2.3 times the two pound value. The experimental apparatus did not allow collapse of the model with $F_y' = 8$ pounds.

In this model the secondary springs had been removed so as to make it collapsible under its equivalent weight of 5.9 pounds.

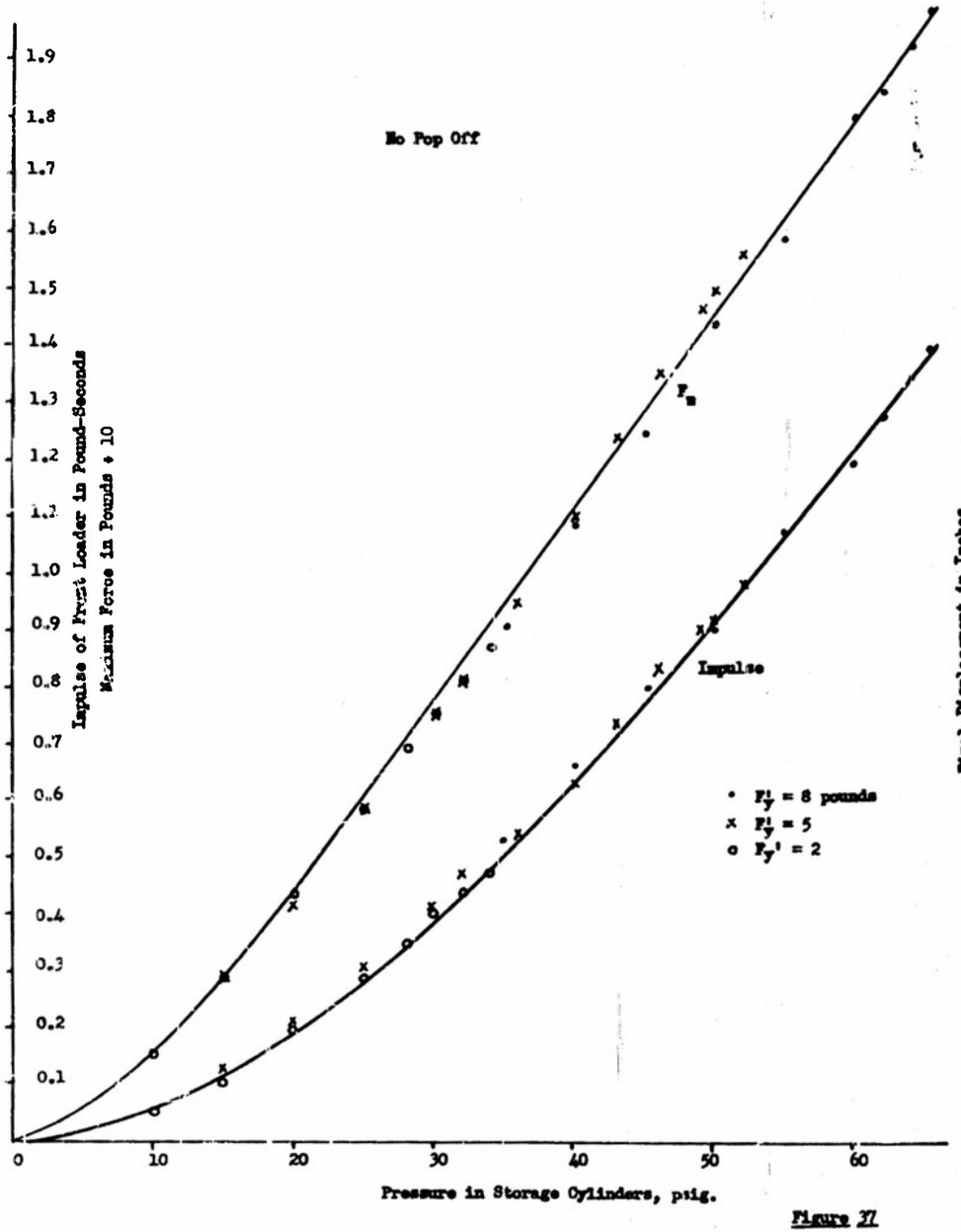

Figure 37

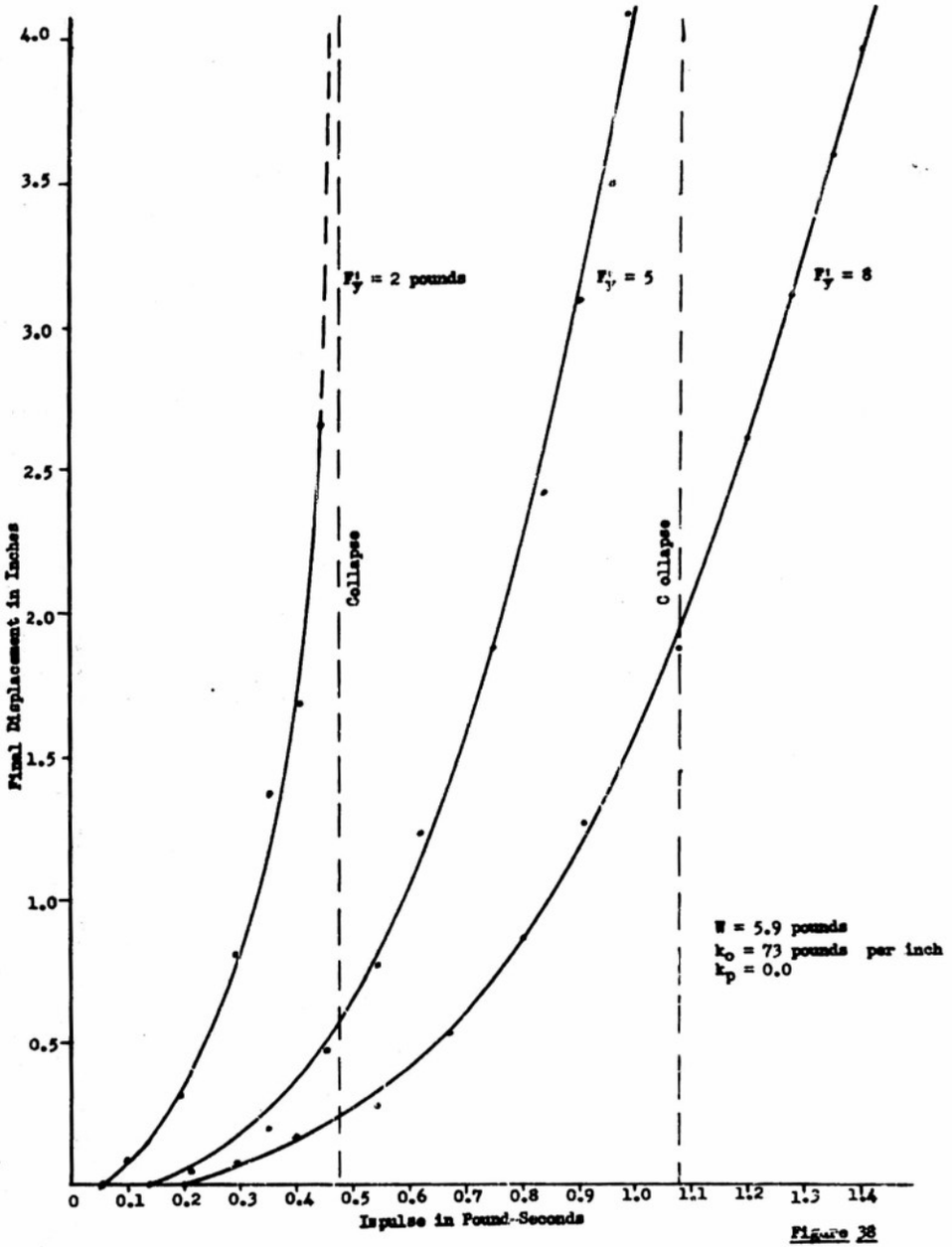

Figure 38

FIGURE 39

Proposed modification of the model to produce elastic couplings between all stories.

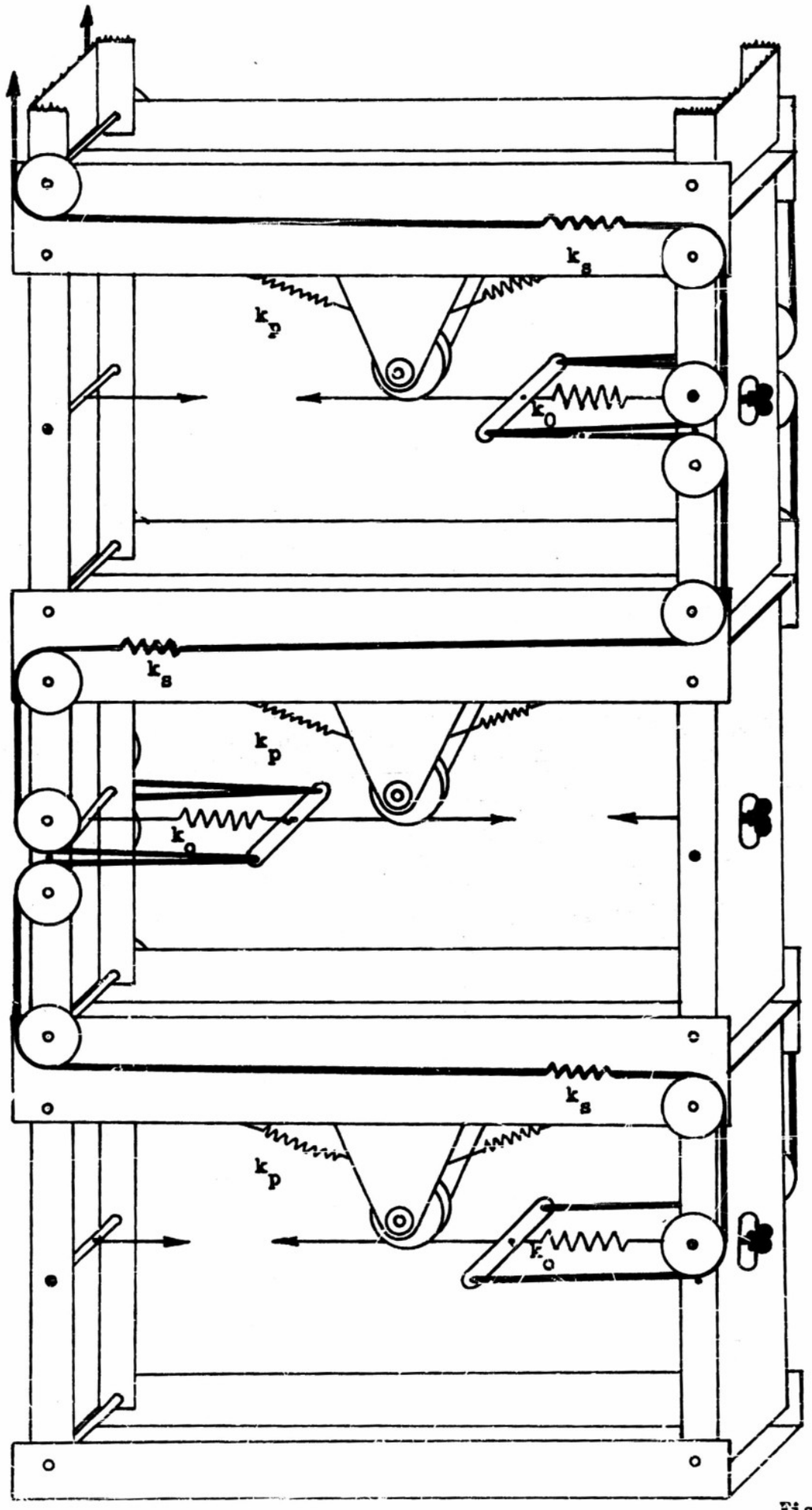

Figure 39

Figure 32

APPENDIX I

Proposed Modification of the Model to Produce Elastic Couplings Among All Stories.

Figure 39 gives a sketch of the usual model, showing three stories now interconnected by one system of pulleys and elastic strings. The pulley-string system, referred to as the right hand system, has an identical counterpart, the left hand system, which is not shown in order that the sketch may be as clear as possible.

Assume that the k_o and k_p values are given for all stories and that the tensile stiffnesses of the strings, k_s, are all alike.

If the first story experiences an elastic displacement to the left of say 1 inch, its right hand k_o spring will be stretched 1/2 inch in addition to the initial stretch, and its left hand k_o spring will be stretched 1/2 inch less than initially. The whiffle-tree of the right hand k_o spring will then exert a pull in the two elastic strings k_s that will be transmitted over the four pulleys and by a second wiffle-tree to the left k_o spring of the second story.

If the string is inextensible, that is if k_s approaches infinity, the displacement of the left k_o spring in the second story due to the string pull will be -1/2 inch, and therefore will be the same as the displacement of the left k_o spring in

the first story; consequently the elastic slopes of the two stories will be identical.

But if the string is elastic, the displacement of the left k_o spring in the second story will be less than the displacement of the left k_o spring in the first story; consequently the elastic slope in the second story due to the string pull will be less than the one in the first story.

Continuing to follow the course of the displacement from the left k_o spring of the second story through the elastic string over four pulleys to the right k_o spring of the third story, we notice that "slackness" rather than tautness results. At this point it becomes necessary to consider the behavior of the counterpart, left hand, pulley-string system not shown in the sketch. This system will experience "slackness" in the first and second stories, but tautness in the third story when the elastic displacement of the first story is to the right. The two counterpart systems of pulleys and elastic strings will therefore transmit a slope of the first story with diminishing magnitude to the stories above. Similarly the two systems of pulleys and strings will couple any one story to all the other stories. The degrees of coupling will depend on the various k_s values.

When the "elastic limit" of a story is reached the friction brake will slip. Consequently the pulley-string systems, being attached to the slipping brake, will not suffer plastic displacements. In other words, the pulley-string coupling is purely elastic.

It is therefore possible to identify the properties of the modified model with those of a building in which the girders are of finite stiffnesses. Thus, for infinitely stiff girders, k_s must be zero, while for very flexible girders, k_s must be very large.

The pulley-string system modification of the model has not been tried out yet. It is possible that secondary effects, due to angularity of the frame at large distortions and due to the appreciable pulley size required by the string, may cause some difficulties, but an encouraging practical aspect of the design is the fact that the k_s values of the strings stands in some inverse relationships to the stiffnesses of the girders in the prototype.

APPENDIX II

Testing Precautions and Model Maintenance

GENERAL

Primarily there are two basic types of necessary precaution. First we must take care that we do not damage any part of the model or any part of the loader system; second we must observe certain procedures in order to obtain accurate tests.

THE MODEL AND THE LOADERS

Incautious testing can result in damage to the model spring systems, the friction brakes, and the loader cylinders, pistons, piston rods, dynamometers, and the displacement potentiometers.

Collapse

If the model is allowed to collapse without any system being present to catch it, some of the main spring support wires are likely to break. Even without breakage of the wires, the main springs can be stressed beyond their elastic limit; this may change their spring constants and perhaps damage the strain gauges. Damage may also occur to the displacement potentiometers.

The support wires may break within the brakes and thereby score the brake bearing systems.

All this can be overcome by the use of stops located so as to prevent the model from being distorted beyond a certain point. The location of these stops, of course, will be such as not to

interfere with tests in which the model does not collapse.

Incorrect Forces

Care must be exercised in applying forces to the model. In particular very high pressure, slowly bleeding forces can buckle the piston rods and score the pistons and cylinders. Some of the loader valves admitting air to the storage cylinders may inadvertently not be completely closed. If this occurs on a loader which is not being used, this loader might be fired with the above results. Hence prior to any test, all the loaders should be checked to see that they have the correct pressure.

Model Maintenance

Very little maintenance is ordinarily required, the main precaution being to keep the model dust free so as to prevent foreign matter from entering the friction brakes. Should the brakes require attention, the following procedure is recommended: the brass brake drum must be refaced in a lathe, along with the masonite brake shoes. Then the shoes are lapped into the drum using a course valve grinding compound ("Cloverleaf" brand, grade C). This scores both drum and shoe circumferentially and greatly aids radial alignment. Then lapping with very fine compound is carried out. Next both shoe and drum are thoroughly cleaned with CCl_4, and the surfaces are now lapped without any compound followed by a lapping using powdered graphite. The excess graphite is removed with CCl_4, care being taken not to remove the desired thin graphite layer on brake and shoe. The

brake is then assembled and placed in the model where it is further worked (about 100 times) under heavy brake spring compression.

Loader Maintenance

The pistons and cylinders are lubricated liberally with powdered graphite. No other type of lubricant should be used since it will greatly increase the model damping introduced by the loaders. Note that even under the best conditions, much of the model damping is introduced by the loaders.

Every two months or so all loaders should be checked to see if the pistons and cylinders are clean and smooth (they will not appear clean owing to the graphite). If they require attention, clean both cylinder and piston with CCl_4 and re-lubricate.

When air leaks develop in the system, it is essential that care be taken not to allow any pipe dope to be introduced into the solenoid valves since this will cause them to stick. If sticky valves occur, they must be disassembled and cleaned with CCl_4.

The solenoid valves' gaskets will occasionally unseat themselves. In this case remove the top of the valve, pop the ball out using air pressure and reseat the gasket with small tweezers.

Elastic bands may be used to make the valves close when de-energised, since residual magnetism keeps the solenoid plunger in the open position. At high pressures (around 60 psi), however, it may be found that the valves will not open properly, in which case it is necessary to remove the elastic bands and close the valves manually.

OBTAINING ACCURATE TESTS

In order to obtain accurate tests, we must be able to set the data accurately into the model, or at least be able to determine the data that we do have. In addition, certain procedures during testing must be observed. In the following it is assumed that all necessary recording equipment has been accurately calibrated.

Applied Forces

Unfortunately the recording system used is subject to considerable overshoot for rapidly varying transients. Hence the forces used should rise slowly, and not have sharp peaks. It has been found that this requires that the pop-off valves not be used if accurate force records are required.

Setting the Main Springs' Spring Constants

The main strings can be set to their desired spring constant fairly easily by using a dial indicator to measure the displacement of the floor in question and by applying a force via a dead weight and pulley system to the same point. The spring constant of the leaf springs are adjustable by raising or lowering the point of attachment of the spring support wires at the end screws of the springs. Note that the initial spring tension affects the spring constant value slightly, and that this tension should be sufficient to prevent any spring from ever relaxing.

Setting the Yield Forces

Unfortunately, there is an appreciable change in the brake characteristics with model motion, hence the brakes must be set

dynamically. Furthermore, the brakes must be reset everytime the model loading is changed if it is desired to preserve the same yield force. First some loading must be decided upon. To obtain a first approximation, block the entire model, and adjust the loaders until the desired loads are obtained, noting various loader pressures and valve settings which now will be kept constant. This is an approximation since, even with the same loader pressures and valve settings, the applied forces will vary with the model's motion. This is particularly true of the rear loads, though not so much of the front and top.

Since, with multi-storied models, changing one brake changes the motion of the other floors and hence the other yield points, the brakes cannot be set individually.

First the brakes are set approximately where one might expect they should be, using a strictly qualitative estimate of what the various floor velocities may be under the given forces. Then the given forces are applied, and the resulting brake force records are observed. It is important to observe the following procedure prior to any test: each floor should be moved back and forth manually 4 or 5 times past yielding so as to help ensure smooth brake action. Otherwise the brakes show a tendency to "freeze" and as a result may chatter. Precautions against damage from collapse should be strictly observed here, since we really have only a crude idea of what the building may do. Then we reset <u>all</u> brakes in a direction to reduce the difference between the actual yield forces and the desired forces. This iterative process

is repeated until the desired yield points have been achieved.

Actual Testing

During an actual test, it is desirable to obtain dynamic records of all measurable quantities involved, namely the applied forces, the brake forces, and the displacements. Since small variations from test to test can be expected, all such quantities should be recorded two or three times.

Since with the present equipment only two force recording channels are available, it can be seen that a given test must be repeated a number of times in order to obtain records of all the quantities. This requires a reasonable assurance that the tests will repeat themselves - as they must if the model is to be of practical use.

The time required to carry through a complete test including calibration of the recording equipment and setting of the springs and brakes is of the order of 4 - 6 hours. This figure naturally depends upon the operator's degree of experience with the equipment.

DESCRIPTION OF ELECTRICAL EQUIPMENT, OPERATING AND MAINTENANCE INSTRUCTIONS

A laboratory memorandum has been prepared on the above two subjects. It is necessarily of a detailed nature and will be available to readers whose interest in the subject is considerable.

Chief of Naval Research
Navy Department
Washington 25, D. C.
Attn: Code 438 2

Director, Naval Research Laboratory
Washington 25, D. C.
Attn: Technical Information Officer 9
Code 500, Mechanics Division 1

Director
Office of Naval Research
Branch Office
1000 Geary Street
San Francisco 9, Calif. 2

Office of Assistant Naval Attache for Research
Naval Attache
American Embassy
Navy No. 100
Fleet Post Office
New York, N. Y. 2

Director
Office of Naval Research
Branch Office
1030 E. Green St.
Pasadena 1, Calif. 1

Director
Office of Naval Research
Branch Office
150 Causeway Street
Boston 10, Massachusetts 1

Director
Office of Naval Research
Branch Office
America Fore Building
844 North Rush Street
Chicago, Illinois 1

Director
Office of Naval Research
Branch Office
346 Broadway
New York 13, N. Y. 1

Bureau of Aeronautics
Navy Department
Washington 25, D. C.
Attn: TD-41, Technical Lib. 2
DE-22, Mr. C. W. Hurley 1

Bureau of Ordnance
Navy Department
Washington 25, D. C.
Attn: AD-3, Technical Lib. 2

Bureau of Ships
Navy Department
Washington 25, D. C.
Attn: Director of Research 2
Code 332 1
Code 442 1

Bureau of Yards and Docks
Navy Department
Washington, D. C.
Attn: Research Division 2

U. S. Naval Academy
Postgraduate School
Electrical Engineering Dept.
Monterey, Calif. 1

Naval Air Experimental Station
Naval Air Material Center
Naval Base
Philadelphia 12, Pa.
Attn: Head, Aero. Mats. Lab. 1

Department of the Army
Code ENGEB
Office of the Chief of Engineers
Washington 25, D. C. 1

Naval Ordnance Laboratory
White Oak, Maryland
RFD 1, Silver Spring, Md.
Attn: Mr. D. E. Marlowe 1

Naval Ordnance Laboratory
White Oak, Maryland
RFD 1, Silver Spring, Md.
Attn: Dr. C. A. Truesdell 1

Commander
U. S. Naval Ordnance Test Station
Imyokern
China Lake, Calif.
Attn: Code 5564 2

Naval Gun Factory
Washington 25, D. C. 1

Commander
U. S. Naval Ordnance Test Station
Pasadena Annex
3202 East Foothill Blvd.
Pasadena 8, Calif.
Attn: Code P5564 1

David Taylor Model Basin
Washington 7, D. C.
Attn: Structural Mechs. Division 2

Director, Materials Laboratory
New York Naval Shipyard
Brooklyn 1, New York 1

Department of the Army
Chief of Staff
The Pentagon
Washington, D. C.
Attn: Director of Research and Development 1

Office of Chief of Ordnance
Research and Development Service
The Pentagon
Washington, D. C.
Attn: ORDTB 2

Commanding Officer
Watertown Arsenal
Watertown, Massachusetts
Attn: Laboratory Division 1

Commanding Officer
Frankford Arsenal
Philadelphia, Pa.
Attn: Laboratory Division 1

Commanding Officer
Squier Signal Laboratory
Ft. Monmouth, N. J. 1

U. S. Air Forces
Research and Development Division
The Pentagon
Washington, D. C. 2

Air Materiel Command
Wright-Patterson Air Force Base
Dayton, Ohio
Attn: Aircraft Laboratory 1
Intelligence Dept.
Air Documents Div. 1

U. S. Atomic Energy Commission
Division of Research
Washington, D. C. 1

National Bureau of Standards
Connecticut Ave. at Upton Street N. W.
Washington, D. C.
Attn: Dr. W. H. Ramberg 1

U. S. Coast Guard
1300 F Street N. W.
Washington, D. C.
Attn: Chief, Test and Development Division 1

Dr. W. H. Hoppmann, II
Dept. of Applied Mechanics
Johns Hopkins University
Baltimore, Maryland 1

Naval Advisory Committee
for Aeronautics
1724 F St. N. W.
Washington 25, D. C.
Attn: Material Research
Coordination Group 2

National Advisory Committee
for Aeronautics
Langley Field, Va.
Attn: Mr. E. E. Lundquist 1

Chief, Armed Forces Special
Weapons Project
Pentagon Bldg.
Washington, D. C. 12

Dr. S. Timoshenko
Stanford University
Stanford, California 1

Dr. N. J. Hoff
Dept. Aero Engr. and Applied
Mechanics
Polytechnic Institute of
Brooklyn
55 Johnson St.
Brooklyn 1, N.Y. 1

Dr. N. M. Newmark
Dept. of Civil Engineering
University of Illinois
Urbana, Illinois 1

Dr. J. N. Goodier
Stanford University
Stanford, California 1

Prof. Jesse Ormendroyd
University of Michigan
Ann Arbor, Michigan 1

Professor F. K. Teichmann
Dept. of Aero Engineering
New York University
Bronx, New York

Professor Bruce G. Johnston
Dept. of Structural Engr.
University of Michigan
Ann Arbor, Michigan 1

Dr. R. D. Mindlin
Dept. of Civil Engineering
Columbia University
Broadway at 117th St.
New York, N. Y. 1

Professor W. J. Krefeld
Dept. of Civil Engineering
Columbia University
Broadway at 117th St.
New York, N.Y. 1

Professor F. L. Bisplinghoff
Dept. of Aero Engineering
Mass. Inst. of Technology
Cambridge 39, Mass. 1

Dean Terman
School of Engineering 1

Additional copies for Project
leader and assistance, Office
of Research Coordination
and reserve for future
requirements 21

Engineering Library
Stanford University 1

Ames Aeronautical Lab.
Attn: Technical Librarian
Moffett Field, Calif. 1

NACA
Attn: Chief, Office of Aero.
Intelligence
1724 F. St. N. W.
Washington 25, D. C. 1

Dr. C. B. Smith
Dept. of Mathematics
Walker Hall
University of Florida
Gainesville, Florida 1

National Advisory Committee
for Aeronautics
1724 F. St. N. W.
Washington 25, D. C.
Attn: Mat. Res. Coord. Group 1